Redistribution of NORTIA in response to pollen tube arrival facilitates fertilization in *Arabidopsis thaliana*

Jing Yuan[1,2*], Yan Ju[1,2*], Daniel S. Jones[4,5], Weiwei Zhang[2,3], Noel Lucca[1,2], Christopher J. Staiger[1,2,3], and Sharon A. Kessler[1,2,**]

[1]Department of Botany and Plant Pathology, Purdue University, West Lafayette, Indiana USA

[2]Purdue Center for Plant Biology, Purdue University, West Lafayette, Indiana USA

[3]Department of Biological Sciences, Purdue University, West Lafayette, Indiana USA

[4]Biology Department, The University of North Carolina at Chapel Hill, Chapel Hill, North Carolina USA (current address)

[5]Department of Microbiology and Plant Biology, University of Oklahoma, Norman, Oklahoma USA

*These authors contributed equally

** Corresponding author

Email: sakessler@purdue.edu

Abstract

During gamete delivery in *Arabidopsis thaliana*, intercellular communication between the attracted pollen tube and the receptive synergid cell leads to subcellular events in both cells culminating in the rupture of the tip-growing pollen tube and release of the sperm cells to achieve double fertilization. Live imaging of pollen tube reception revealed dynamic subcellular changes that occur in the female synergid cells. Pollen tube arrival triggers the trafficking of NORTIA (NTA) MLO protein from Golgi-associated compartments and the accumulation of endosomes at or near the synergid filiform

apparatus, a membrane-rich region that acts as the site of communication between the pollen tube and synergids. Domain swaps and site-directed mutagenesis suggest that NTA's C-terminal cytoplasmic tail with its calmodulin-binding domain regulates NTA movement and function in pollen tube reception. Signal-mediated trafficking of NTA to the filiform apparatus upon pollen tube arrival may facilitate intercellular communication that leads to pollen tube rupture.

Introduction

Intercellular communication is central to the proper development and maintenance of all multicellular organisms. During this communication, signals from one cell are perceived by receptors in another cell and translated into various subcellular responses. These include signal transduction cascades leading to transcription of other genes, calcium signaling, and trafficking of proteins to different organelles or regions of the cell. A well-studied example of signal-induced protein trafficking in plant development is the redistribution of the PIN polar auxin transporters to different sides of the cell during important developmental events such as embryo patterning, leaf initiation and lateral root initiation (Petrasek et al., 2006; Naramoto, 2017; Salanenka et al., 2018). In plants, most intercellular communication occurs between cells that are genetically identical and connected by adjoining cell walls. One exception is pollination, in which pollen (the male gametophyte) is released from an anther, transported to a receptive stigma, and produces a tip-growing pollen tube that grows through the female tissues of the pistil and delivers the two sperm cells to the female gametophyte (also known as the embryo sac, Fig 1A). The pollen tube's journey through the pistil requires cell-to-cell interactions

52 with the female that allows water and nutrient uptake and enables the detection of cues
53 important for guidance toward the female gametes (Johnson et al., 2019).
54
55 In the model plant *Arabidopsis thaliana*, complex signaling events ranging from pollen
56 landing on the stigma to fusion of gametes occur over several hours. Most of our
57 knowledge about the signaling pathways involved along the pollen tube's journey
58 through the female is limited to the final stages of pollination and involve a highly
59 specialized pair of female gametophyte cells known as synergids. During female
60 gametophyte development, meiosis followed by three rounds of mitosis produce the egg
61 cell and central cell along with 2 synergid cells flanking the egg cell and 3 antipodal cells
62 on the chalazal end of the embryo sac (Drews and Yadegari, 2002), Fig 1A). The
63 synergid cells are accessory cells that control the behavior of the pollen tube during the
64 final stages of pollination. Before pollen tube arrival, they secrete cysteine-rich LURE
65 peptides that act as short-range pollen tube attractants that are recognized by receptor-
66 like kinases in the tip of the pollen tube to regulate the direction of pollen tube growth
67 and guide the pollen tube to the micropyle of the ovule (Okuda et al., 2009; Takeuchi
68 and Higashiyama, 2016; Wang et al., 2016). After pollen tube arrival, the synergids
69 communicate with the pollen tube to induce changes that result in pollen tube rupture
70 and delivery of the sperm cells (Kessler and Grossniklaus, 2011; Johnson et al., 2019).
71 Thus, synergids are critical for ensuring that double fertilization can occur to produce
72 seeds.
73

74 In Arabidopsis, live imaging has been used to examine the behavior of both the pollen
75 tube and the synergids during the process of pollen tube reception. A pollen tube
76 follows the gradient of LURE attractants, enters the micropyle of the ovule, and pauses
77 its growth for 30 min to 1 h just outside the receptive synergid (Iwano et al., 2012;
78 Denninger et al., 2014; Ngo et al., 2014). During this pause in pollen tube growth,
79 communication occurs between the pollen tube and the synergids that leads to
80 subcellular changes and ultimately to the death of both the pollen tube and the receptive
81 synergid. Cytoplasmic calcium ($[Ca^{2+}]_{cyto}$) oscillations occur in both the tip of the pollen
82 tube and in the 2 synergid cells during this communication phase. $[Ca^{2+}]_{cyto}$ levels
83 continue to increase in both cell types until the pollen tube starts to grow again and
84 bursts to release the sperm cells, a catastrophic event for both the pollen tube and the
85 receptive synergid, which also degenerates (Iwano et al., 2012; Denninger et al., 2014;
86 Ngo et al., 2014). Mutations in genes that regulate communication between the
87 synergids and pollen tube during pollen tube reception result in a pollen tube
88 overgrowth phenotype in which the pollen tubes are attracted normally to the ovules, but
89 do not get the signal to burst and release the sperm cells. Presumably, synergid-
90 induced changes in the cell wall of the pollen tube tip do not occur in these mutants,
91 therefore the pollen tube continues to grow and coil inside the embryo sac. Synergid-
92 expressed genes that participate in pollen tube reception include the FERONIA (FER)
93 receptor-like kinase, the GPI-anchored protein LORELEI (LRE), and the Mildew
94 Resistance Locus-O (MLO) protein NORTIA (NTA, also known as AtMLO7) (Escobar-
95 Restrepo et al., 2007; Capron et al., 2008; Kessler et al., 2010; Ngo et al., 2014; Li et
96 al., 2015; Liu et al., 2016). Mutations in all of these genes lead to the pollen tube

97 overgrowth phenotype due to disruption of the pollen tube-synergid communication
98 pathway.
99
100 FER and LRE are necessary for the calcium oscillations that occur in synergids in
101 response to pollen tube arrival (Ngo et al., 2014). In contrast, *nta-1* mutants have
102 $[Ca^{2+}]_{cyto}$ oscillations at lower amplitudes, indicating that NTA may participate in
103 modulating Ca^{2+} fluxes in the synergids during communication with the pollen tube and
104 likely acts downstream of FER and LRE (Ngo et al., 2014). Like all members of the MLO
105 gene family, NTA has seven membrane-spanning domains and a predicted calmodulin-
106 binding domain (CaMBD) in its C-terminal intracellular tail (Devoto et al., 2003; Kusch et
107 al., 2016). Calmodulin (CaM) is a small protein that binds Ca^{2+} and is involved in signal
108 transduction for many cellular processes (Yang and Poovaiah, 2003). We previously
109 showed that the C-terminal domain of NTA is necessary and sufficient for MLO function
110 in pollen tube reception (Jones et al., 2017), but the significance of the CaMBD in pollen
111 tube reception remains an open question.
112
113 The subcellular localization of these important pollen tube reception proteins is not
114 always predictive of their function in communicating with the pollen tube. As expected
115 for early response proteins, both FER and LRE are expressed in synergid cells where
116 they localize in or near a specialized region called the filiform apparatus, a membrane
117 rich area located at the micropyle end of the synergids (Huck et al., 2003; Rotman et al.,
118 2003; Escobar-Restrepo et al., 2007; Capron et al., 2008; Li et al., 2015; Lindner et al.,
119 2015; Liu et al., 2016). The filiform apparatus is thought to be important for the secretion

120 of attractant peptides and is the first site of interaction between the pollen tube and
121 synergid cell prior to pollen tube reception (Mansfield et al., 1991; Huang and Russell,
122 1992; Leshem et al., 2013). In contrast, before pollen tube arrival, NTA is sequestered
123 in a Golgi-associated compartment within the synergid cell and excluded from the
124 filiform apparatus region (Jones et al., 2017). At the end of pollen tube reception, NTA
125 protein is only detected in the region of the filiform apparatus, indicating that this protein
126 changes its subcellular localization during pollen tube reception (Kessler et al., 2010).
127 This suggests that pollen tube-triggered regulation of the synergid secretory system
128 may be a crucial subcellular response to pollen tube arrival and that NTA function may
129 be related to its subcellular distribution; however, the precise timing and significance of
130 NTA's redistribution are still unclear.
131
132 In this study, we take advantage of a live-imaging system to further characterize
133 synergid cellular dynamics during pollen tube reception and to determine the timing and
134 significance of the polar redistribution of NTA to the filiform apparatus. To investigate
135 the link between Ca^{2+} and MLO function in pollen tube reception, we assayed the
136 influence of the CaMBD on NTA's function and subcellular distribution through C-
137 terminal truncations and a point mutation disrupting the CaMBD. We show that the polar
138 redistribution of NTA is triggered by the approach of a pollen tube, is important for
139 pollen tube reception, and is regulated by the CaMBD. While most subcellular
140 compartments remain distributed throughout the synergid cells during pollen tube
141 reception, recycling endosomes respond to pollen tube arrival by accumulating towards
142 the filiform apparatus. Moreover, we show that targeting NTA to the filiform apparatus

143 before pollen tube attraction does not induce synergid cell death.

144

145 **Results**

146 **Time-lapse imaging of NORTIA redistribution using a semi-*in vivo* assay**

147 Pollen tube reception is a complex process that requires the synergid cells to recognize
148 the approaching pollen tube and to send signals back to the pollen tube that result in
149 release of the sperm cells at the correct time and place. We previously showed that the
150 NTA-GFP fusion protein localizes to a Golgi-associated compartment of the synergids
151 before pollen tube attraction (Jones et al., 2017). When imaged after pollen tube
152 reception, NTA-GFP is concentrated at the micropylar end of the synergid (in or near
153 the filiform apparatus) (Kessler et al., 2010). NTA-GFP doesn't accumulate near the
154 filiform apparatus in *fer* ovules with pollen tube overgrowth, suggesting that FER-
155 mediated signaling that occurs during pollen tube reception triggers NTA-GFP
156 redistribution that in turn contributes to the interaction of the synergid with the pollen
157 tube (Kessler et al., 2010). An alternative hypothesis is that pollen tube rupture triggers
158 NTA-GFP redistribution and is a symptom of pollen tube reception rather than an
159 important contributor to the signaling pathway. To distinguish between these two
160 possibilities, we used a semi-*in vivo* pollination system combined with spinning disk
161 confocal microscopy to determine the timing of NTA-GFP redistribution during the pollen
162 tube reception process. In the semi-*in vivo* system, pollen tubes grow out of a cut style
163 and are attracted to ovules arranged on pollen germination media (Palanivelu and
164 Preuss, 2006). This system has previously been used to quantify and track pollen tube
165 attraction to ovules and to image ($[Ca^{2+}]_{cyto}$ reporters during pollen tube reception

166 (Hamamura et al., 2011; Hamamura et al., 2012; Denninger et al., 2014; Hamamura et
167 al., 2014; Ngo et al., 2014). In order to follow subcellular changes in NTA-GFP protein
168 localization before, during, and after pollen tube arrival, we used pollen from plants
169 expressing the pollen-specific AUTOINHIBITED Ca^{2+}-ATPASE9$_{pro}$::DsRed
170 (ACA9$_{pro}$::DsRed) reporter and ovules expressing NTA$_{pro}$::NTA-GFP in the semi-*in vivo*
171 system. Approximately 4 h after pollination, pollen tubes emerged from the style onto
172 the media and were attracted to ovules (Fig 1B). Images in the red and green channels
173 were collected every 5 min from when a pollen tube approached an ovule until after the
174 pollen tube ruptured inside the ovule. In our system, most of the ovules displayed
175 successful pollen tube attraction and reception, while others did not attract a pollen tube
176 during the time course of the imaging experiments (Fig 1B and S1). A second group
177 were imaged under the same conditions and serve as a negative control for
178 environmentally-induced changes in NTA-GFP localization. 83% of the ovules that
179 attracted a pollen tube that successfully burst to deliver the sperm cells (n=93)
180 displayed NTA-GFP redistributed to the micropylar end of the synergid cell (Fig 1C-E).
181 Ovules without NTA-GFP redistribution displayed abnormal pollen tube behavior in
182 which pollen tubes were attracted but stopped growing and never ruptured to release
183 the sperm cells. Neighboring ovules that did not attract a pollen tube (n=103) but were
184 imaged under the same semi-*in vivo* conditions did not have redistribution of NTA-GFP
185 (Fig 1E), nor did ovules that were incubated on pollen germination media without a
186 pollinated pistil (n=133, Fig 1E). These data suggest that pollen tube arrival is
187 necessary for NTA-GFP redistribution and that the imaging conditions do not trigger
188 redistribution (Fig 1E).

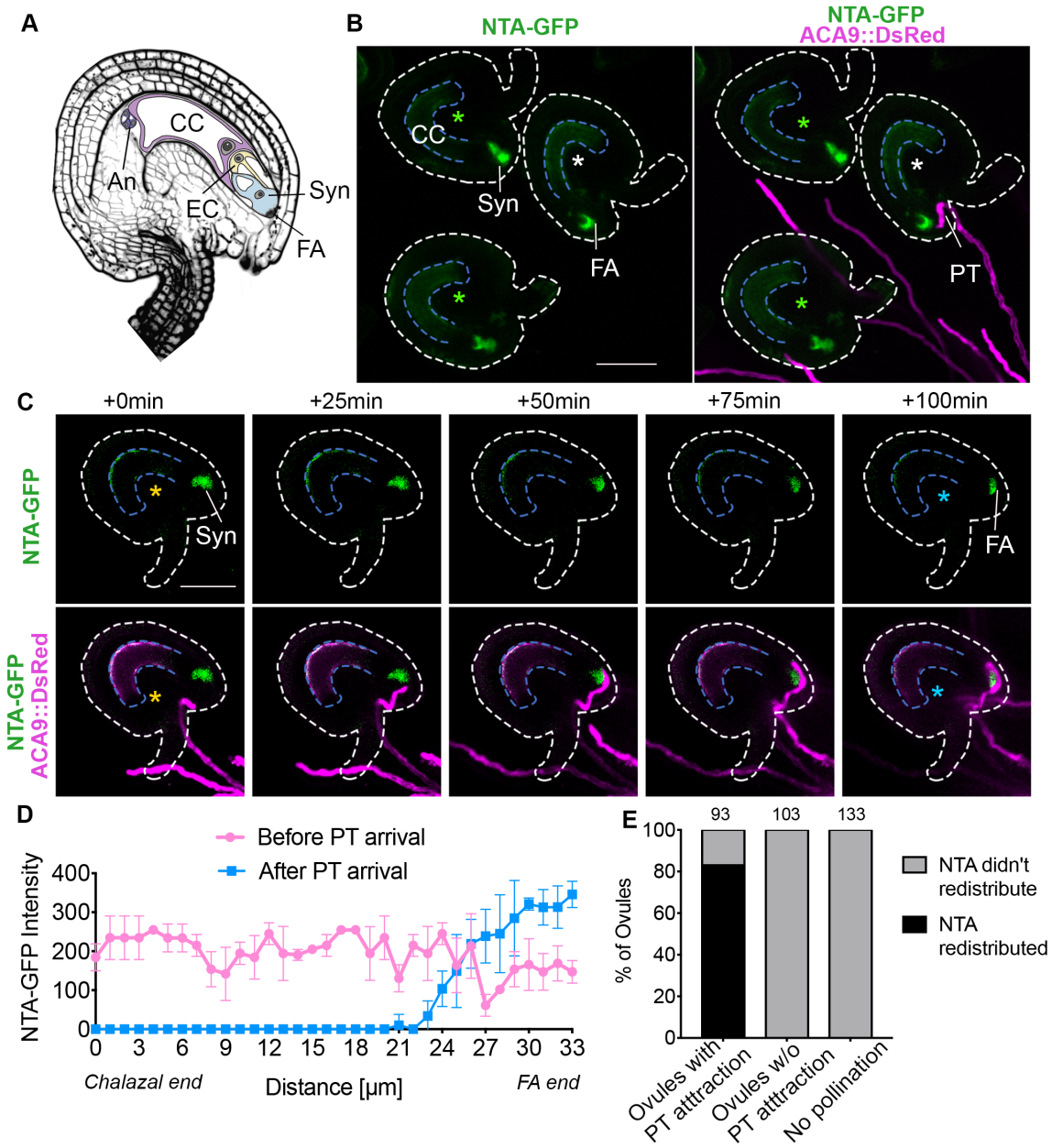

189

Figure 1. NTA redistributes to the filiform apparatus region as the pollen tube approaches. (A) Diagram of a mature *Arabidopsis thaliana* ovule and embryo sac, modified from Jones et al, 2018. (B, C) Live imaging of pollen tube (PT) reception using NTA-GFP labeled synergids (green signal) and ACA9::DsRed pollen tubes (magenta signal). (B) NTA-GFP redistribution occurred in ovules that attracted a pollen tube (ovules with white stars), while NTA-GFP redistribution did not occur in ovules without pollen tube attraction (ovules with green stars). (C) Time-lapse imaging of NTA-GFP movement during pollen tube reception. NTA-GFP before (ovules with yellow stars) and after (ovules with blue stars) the PT resumes growth after initial arrival at the filiform apparatus. (D) Quantification of NTA-GFP signal before (yellow starred ovule) and after (blue starred ovule) pollen tube arrival. Synergid cell from chalazal end to filiform apparatus (FA) end was defined from 0 to 33 µm in length. (E) Quantification of the percentage of ovules with NTA redistribution under different experimental conditions. Bars=50µm (A, C). CC, Central Cell; Syn, Synergid Cells; EC, Egg Cell; An, Antipodal cells; FA, Filiform Apparatus; PT, Pollen Tube.

190

191 Our semi-*in vivo* system also allowed us to determine the timing of NTA-GFP
192 redistribution in relation to the position of the pollen tube as it approached the synergids.
193 We defined the 0 min timepoint as the time where the pollen tube just reached the
194 micropylar opening of the ovule (Fig 1C, ovules with yellow stars, Movies S1 and S2). In
195 all cases, NTA-GFP movement also started from this time point. During the following
196 30–50 min, pollen tubes grew through the micropyle region of ovule and arrived at the
197 filiform apparatus of the receptive synergid cell. During this time, three quarters to half
198 of the NTA-GFP signal moved to the micropylar end of synergid cells, indicating that the
199 approach of the pollen tube triggers NTA-GFP movement. As reported in (Ngo et al.,
200 2014) and (Denninger et al., 2014), the arriving pollen tubes paused their growth
201 outside the filiform apparatus for 30–50 min, presumably for cell-to-cell communication.
202 During this period, NTA-GFP signal continued to move toward the filiform apparatus.
203 The whole movement took around 70–80 min, and after the redistribution completed,
204 pollen tubes resumed growth and ruptured to deliver the sperm cells and complete
205 double fertilization (Fig 1C and Movies S1 and S2). Even though only one of the
206 synergids receives the pollen tube, NTA-GFP was actively redistributed to the filiform
207 apparatus in both synergid cells in response to pollen tube arrival, similar to the
208 activation of $[Ca^{2+}]_{cyto}$ oscillations in both synergids during pollen tube reception
209 reported in (Ngo et al., 2014).
210
211
212

213 **The Golgi apparatus does not concentrate at the filiform apparatus during pollen**
214 **tube reception**

215 We previously determined that NTA is sequestered in a Golgi-associated compartment
216 in synergid cells that have not attracted a pollen tube (Jones et al., 2017) . Our live-
217 imaging data suggests that NTA-GFP is selectively moved out of the Golgi and
218 trafficked to the region of the filiform apparatus in response to pollen tube arrival;
219 however, it is possible that the observed NTA-GFP movement is a result of massive
220 reorganization of subcellular compartments. To distinguish between these possibilities,
221 we investigated the behavior of Golgi in synergid cells during pollen tube reception. We
222 used the semi-*in vivo* imaging system described above with a synergid-expressed Golgi
223 marker (Man49-mCherry) co-expressed with NTA-GFP (Jones et al., 2018). In all
224 replicates, the Golgi marker was distributed throughout the synergids, excluded from the
225 filiform apparatus, and co-localized with NTA-GFP as reported previously (Fig 2A).
226 When a pollen tube approached the synergids, NTA-GFP redistributed to the filiform
227 apparatus region of the synergids as observed previously (Fig 1), but the Golgi-mCherry
228 marker remained consistently distributed throughout the synergid cells and did not
229 concentrate near the filiform apparatus (Fig 2B). In order to examine the behavior of the
230 Golgi during later stages of pollen tube reception, we used the synergid-expressed
231 Golgi marker line (Man49-mCherry) and pollen that was expressing GFP
232 ($Lat52_{pro}$::GFP). In all cases, the Golgi marker remained randomly distributed
233 throughout the synergid cells, even after pollen tube rupture (Fig 2C-D, Movies S3 and
234 S4). These results indicate that the movement of NTA-GFP during pollen tube reception
235 is not linked to mass redistribution of the Golgi apparatus.

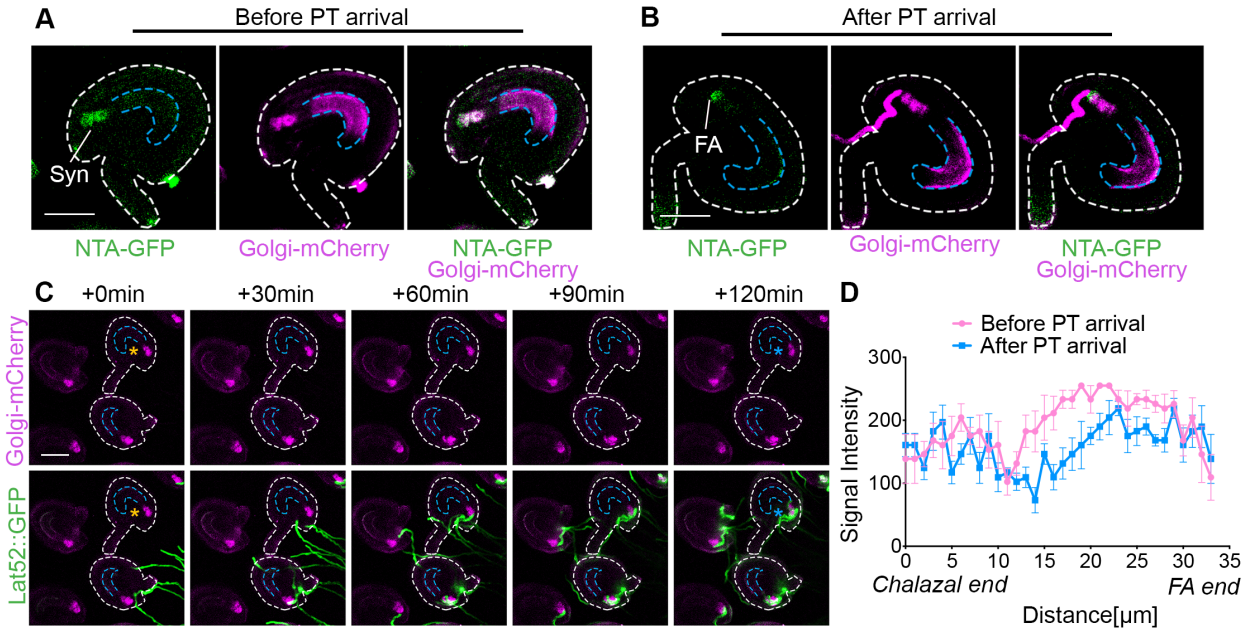

Figure 2. The Golgi marker is randomly distributed throughout synergids during pollen tube reception. (A) NTA-GFP (green signal) and Golgi-mCherry signals (magenta signal) are evenly distributed along the length of the synergid and co-localized within synergid cells before pollen tube arrival. (B) After pollen tube arrival, NTA-GFP redistributed to FA region, but Golgi-mCherry did not redistribute to FA. (C) Live imaging of Golgi-mCherry during reception of Lat52::GFP labeled pollen tubes. (D) Quantification of Golgi-mCherry signal along the length of synergids before (ovule with yellow star in C) and after (ovule with blue star in C) pollen tube arrival. Bars=30μm (A-B), 50μm (C). Syn, Synergid cells, FA, Filiform Apparatus.

Distribution of cellular compartments in synergid cells during pollen tube reception

A signal from the arriving pollen tube seems to trigger the movement of NTA-GFP out of the Golgi-associated compartments. It is possible that pollen tube arrival triggers other changes to synergid subcellular organization. We previously reported the localization of synergid-expressed markers for the ER, peroxisome, endosome and the trans-Golgi Network (TGN) in unfertilized ovules *in vivo* using confocal laser scanning microscopy (Jones et al., 2018). Before pollen tube arrival, SP-mCherry-HDEL (an ER-associated marker), mCherry-SKL (a peroxisome-associated marker), and mCherry-RabA1g (a

248 recycling endosome-associated marker) were all distributed evenly throughout synergid
249 cells (Fig S2 and 3A; (Jones et al., 2018). The TGN-associated marker SYP61 exhibited
250 two types of distribution patterns before pollen tube arrival: in type 1 synergids, the
251 marker accumulated near the filiform apparatus, whereas type 2 synergids displayed a
252 punctate distribution pattern throughout the cells (Fig S2; (Jones et al., 2018). During
253 pollen tube reception, no change was seen in the TGN marker distribution in either type
254 of synergids (Fig S2, C-D, Movies S5 and S6). Likewise, the ER and peroxisome
255 markers maintained a diffuse distribution throughout the synergids and did not
256 accumulate at the filiform apparatus region (Fig S2, A-B and E-F, Movies S7-10). In
257 contrast, we detected a more dynamic behavior of the endosome marker during pollen
258 tube reception. Endosomes are membrane-bound compartments that are involved in
259 the endocytic membrane transport pathway from the plasma membrane to the vacuole.
260 Endosomes also transport molecules from the Golgi and either continue to vacuole or
261 recycle back to the Golgi (Stoorvogel et al., 1991). We previously reported that
262 mCherry-RabA1g is distributed throughout synergid cells and had some overlap with
263 NTA-GFP in synergids of unpollinated ovules (Jones et al., 2018). Using the semi-*in*
264 *vivo* system, we confirmed that before pollen tube arrival, mCherry-RabA1g distributed
265 throughout synergid cells (Fig 3A). Interestingly, as pollen tubes approached, the
266 endosome marker started to accumulate in the filiform apparatus region of the synergid
267 cells (Fig 3A and B). By the time that pollen tube reception was completed, most of the
268 endosome signal was concentrated at or near the filiform apparatus (Fig 3B-D and S3,
269 Movies S11 and S12). These results indicate that the RabA1g endosome compartments

270 have a distinct response to pollen tube arrival and may play a role in facilitating the

271 intercellular signaling pathway that occurs between the synergids and the pollen tube.

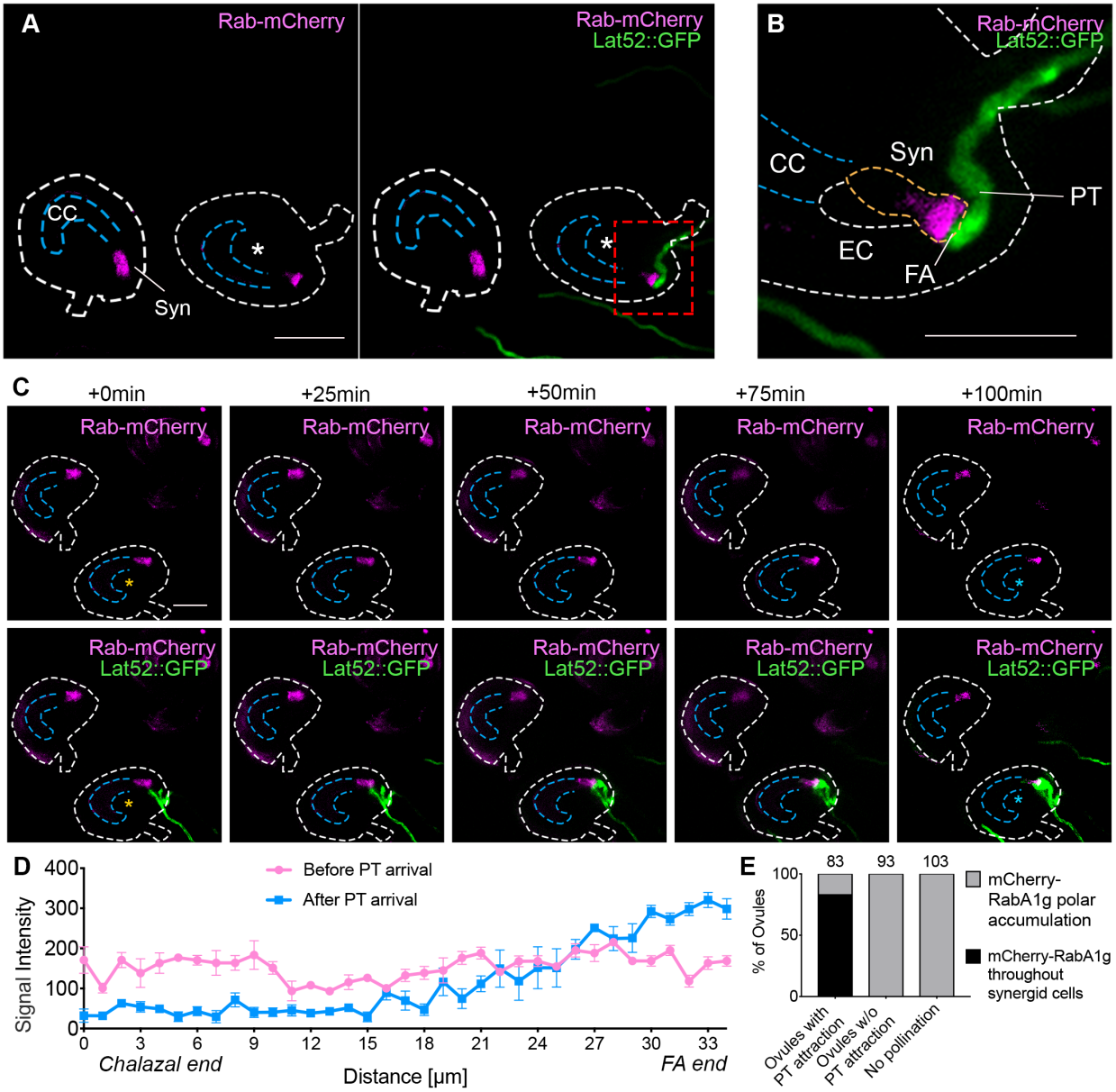

272

Figure 3. Endosome marker polarly accumulates toward filiform apparatus during pollen tube reception. (A) Rab-mCherry endosome marker (magenta signal) accumulates at the FA region in response to pollen tube arrival (ovule with white star). (B) Higher magnification of the micropylar region of starred ovule in (red box in panel A). (C) Timing of Rab-mCherry polar accumulation during pollen tube arrival (ovules with stars). (D) Quantification of Rab-mCherry signal along the length of synergids during pollen tube reception. Bars=50µm. (E) Quantification of ovule percentage with endosome marker throughout the synergids (gray bars) or with polar accumulation near the filiform apparatus (black bars). CC, Central Cell; EC, Egg Cell; Syn, Synergid Cells; FA, Filiform Apparatus; PT, Pollen Tube.

273

274 **The CaMBD is important for NTA's function in pollen tube reception**

275 The timing of the NTA redistribution during pollen tube arrival is similar to the start of
276 synergid $[Ca^{2+}]_{cyto}$ oscillations that are triggered by the pollen tube in a FER-dependent
277 manner (Iwano et al., 2012; Hamamura et al., 2014; Ngo et al., 2014). MLO proteins
278 have the potential to bind Ca^{2+} through calmodulin binding domains (CaMBD) in their C-
279 terminal cytoplasmic tails following the seventh transmembrane domain (Devoto et al.,
280 1999; Kim et al., 2002a; Panstruga, 2005; Consonni et al., 2006). Like all MLO proteins,
281 NTA has a predicted CaMBD in its C-terminal tail (Fig 4A). In *nta-1* mutants, pollen
282 tube-triggered $[Ca^{2+}]_{cyto}$ oscillations occur but at a lower amplitude (Ngo et al., 2014).
283 Domain swaps with MLO8 revealed that the C-terminal tail domain of NTA is necessary
284 and sufficient for MLO-mediated pollen tube reception and important for NTA's
285 subcellular distribution in synergids (Jones et al., 2017). Together, these data suggest
286 that the subcellular distribution of NTA before and during pollen tube reception could be
287 influenced by $[Ca^{2+}]_{cyto}$ levels sensed by the CaMBD. Previous studies have found that
288 CaM-binding activity of the CaMBD influences MLO function in powdery mildew
289 susceptibility (Kim et al., 2002a).

290

291 We hypothesized that CaM-binding activity is also important for NTA's function during
292 pollen tube reception. To test this, a truncation removing the C-terminal tail including the
293 CaMBD ($NTA^{\Delta 450}$), a point mutation in a conserved tryptophan (NTA^{W458A}) necessary for
294 CaM-binding function in other CaMBDs (Arazi et al., 1995; Yamada et al., 1995; Kim et
295 al., 2002b), and a truncation removing the tail immediately following the CaMBD
296 ($NTA^{\Delta 481}$), all fused to GFP, were generated and expressed under the synergid-

297 expressed MYB98 promoter in the *nta-1* background (Fig 4). Ovule counts in
298 homozygous lines revealed that all three constructs had significant reductions in
299 unfertilized ovules compared to *nta-1*. However, only NTA$^{\Delta 481}$ rescued at similar levels
300 as full-length NTA (Fig 4B), indicating that the C-terminal tail after the CaMBD is
301 dispensable for NTA function. Both NTA$^{\Delta 450}$ and NTA^{W458A} partially rescued *nta-1*,
302 suggesting that either removal or disruption of the CaMBD have a similar impact on
303 NTA's function.

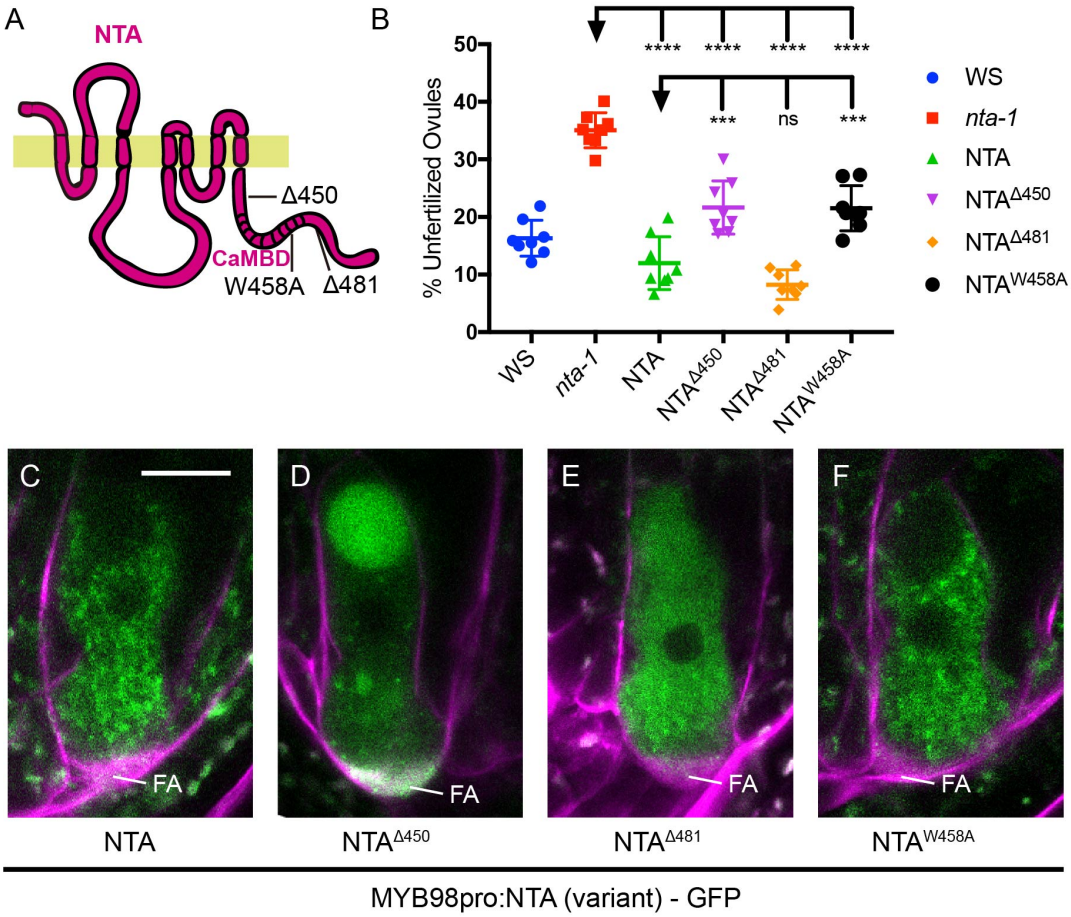

304

305 **Figure 4. Analysis of NTA variants expressed in synergids of *nta-1*.** (A) Diagram of the NTA protein
306 with variant positions indicated. The yellow bar represents a lipid bilayer, with the N-terminal extension predicted to be outside the membrane. (B) Complementation analysis of NTA variants in T2 plants homozygous for MYB98$_{pro}$::NTA(variant)-GFP constructs in *nta-1* mutants. (C-F) NTA (variant)-GFP (green) distribution in synergid cells of unfertilized ovules merged with FM4-64 (magenta). Bars = 10 µm. Adjusted P values from a Student's *t*-test are as follows: **** indicates $P < 0.0001$; *** indicates $P = 0.001$ to 0.0001($P = 0.0009$ when compare between NTA and NTA$^{\Delta 450}$; $P = 0.0005$ when compared between NTA and NTA^{W458A}); and ns indicates $P = 0.0633$. FA, Filiform Apparatus.

307 **A functional CaMBD facilitates NTA accumulation at the filiform apparatus during**
308 **pollen tube arrival**

309 Prior to pollen tube arrival, NTA is distributed throughout the entire synergid cell where it
310 is localized primarily within Golgi (Fig 4C) (Kessler et al., 2010; Jones et al., 2017).
311 When expressed in synergid cells, related MLO proteins that localize within Golgi can
312 rescue *nta-1* whereas those that localize elsewhere do not function in pollen tube
313 reception (Jones et al., 2017). The partial complementation of *nta-1* by the CaMBD-
314 disrupted variants could be due to disrupted localization patterns before and/or after
315 pollen tube arrival. In virgin ovules, both $NTA^{\Delta 481}$ and NTA^{W458A} were distributed
316 throughout the synergid cell in punctate compartments and were predominantly
317 excluded from the filiform apparatus (Fig 4E and F). $NTA^{\Delta 450}$ accumulated in punctate
318 compartments throughout the synergid, but was also detected near the filiform
319 apparatus and in the vacuole (Fig 4D). Although the two variants with disrupted
320 CaMBDs ($NTA^{\Delta 450}$ and NTA^{W458A}) both partially rescued the *nta-1* unfertilized ovule
321 phenotype at similar levels, they had different distributions in the synergid cell. This
322 suggests that differences in localization between these two variants may not be
323 functionally relevant to pollen tube reception. Due to this, we focused primarily on
324 NTA^{W458A} for our downstream analyses and comparisons with wildtype NTA so as to not
325 further complicate the interpretation of our results.
326

327 With "NTA-like" distribution in the synergid cell, we suspected that the NTA^{W458A} variant
328 would accumulate within Golgi-associated compartments similar to wildtype NTA.
329 NTA^{W458A} was co-expressed with fluorescent markers for Golgi (LRE_{pro}::Man49-

330 mCherry, (Liu et al., 2016)) and the TGN (MYB98pro:Syp61-mCherry,(Jones et al.,
331 2017)) in synergid cells and virgin ovules were analyzed via CLSM (Fig S4). The
332 NTA^{W458A} variant partially co-localized with the Golgi maker (Fig S4A) and had no
333 overlap with the TGN marker (Fig S4B), similar to wildtype NTA localization(Jones et al.,
334 2017). These data demonstrate that neither NTA's distribution within the synergid cell,
335 where it is maintained out of the filiform apparatus prior to pollen tube arrival, nor its
336 localization within Golgi-associated compartments are dependent on a functional
337 CaMBD.
338
339 During pollen tube reception, NTA is actively redistributed toward the filiform apparatus
340 region. The NTA^{W458A} variant maintains a wildtype distribution and localization pattern in
341 synergids without pollen tubes but does not fully rescue *nta-1*'s unfertilized ovule
342 phenotype. To test whether the CaMBD is important for NTA's redistribution in response
343 to pollen tube arrival, the semi-*in vivo* system described above was used to monitor
344 NTA^{W458A} movement in the *nta-1* background. In this background, the partial rescue by
345 NTA^{W458A} leads to some ovules having normal pollen tube reception, while others
346 exhibit pollen tube overgrowth and a failure of pollen tube rupture. In the semi-*in vivo*
347 system, NTA^{W458A} ovules that did not attract a pollen tube, maintained distributions
348 outside of the filiform apparatus, consistent with unpollinated flowers above (Fig S5A
349 and C). In ovules with successful pollen tube reception, NTA^{W458A} redistributed to the
350 filiform apparatus region, but in many cases this redistribution was not as complete as
351 with the wild-type NTA-GFP protein, with some GFP signal remaining outside the
352 filiform apparatus region (Fig 5 and Fig S5, B and D). In ovules where pollen tube

353 reception was not successful due to pollen tube overgrowth, NTA^{W458A} did not

354 accumulate at the filiform apparatus region of the synergids (Fig 5C). These data

355 suggest that an active CaMBD enhances NTA's redistribution to the filiform apparatus

356 region during pollen tube reception and that NTA redistribution is correlated with pollen

357 tube rupture.

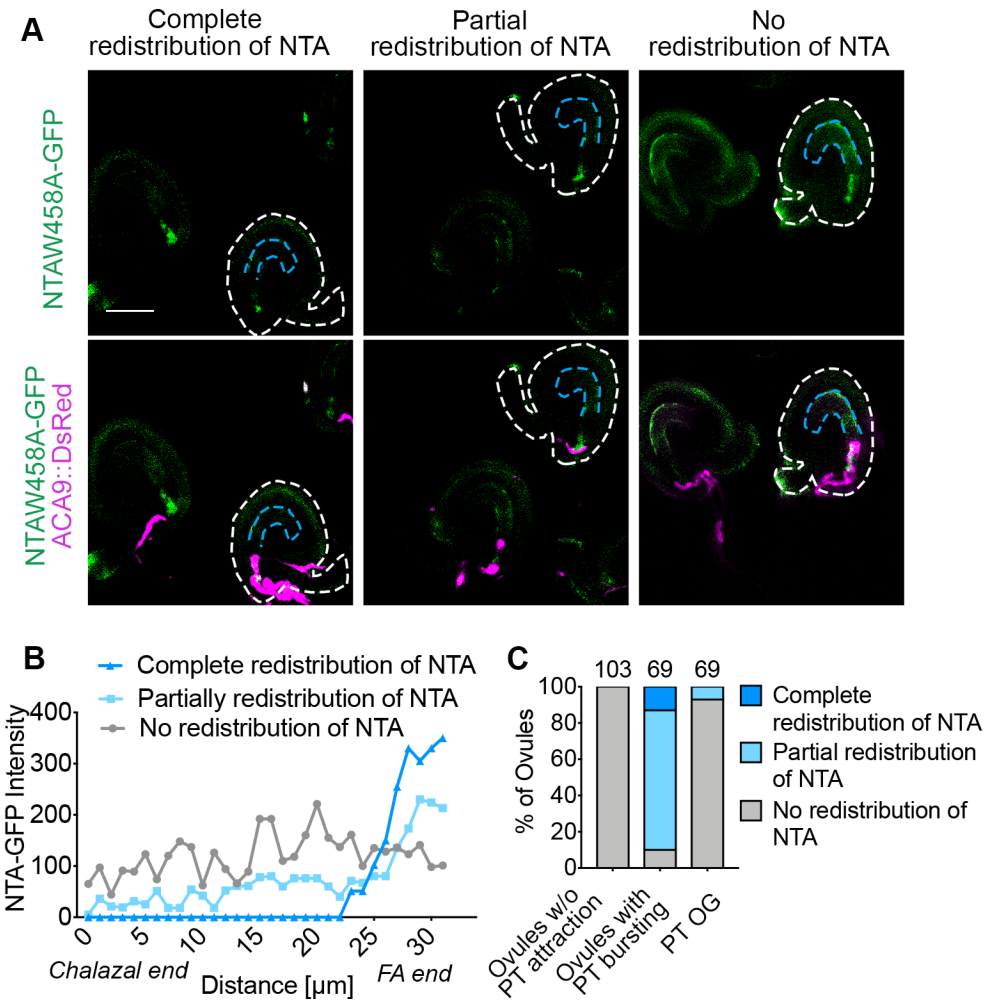

358

359 **Figure 5. A point mutation in the CaMBD (NTA^{W458A}) affects redistribution and pollen tube reception.** (A) NTA^{W458A} has 3 different localization patterns in response to PT arrival under semi *in-vivo* conditions. (B) Quantification of GFP signal intensity in NTA^{W458A} synergids during pollen

360 tube reception. (C) Analysis of NTA^{W458A}-GFP distribution patterns in ovules with successful (PT bursting) and unsuccessful (no PT or PT overgrowth (PT OG)) pollen tube reception. Bar=50 µm

361

362 **Premature distribution of NTA to the filiform apparatus region is not toxic to**
363 **synergid cells**
364 The selective targeting of NTA-GFP from the Golgi apparatus to the filiform apparatus
365 region of the synergid cells during pollen tube arrival (Fig 1-2) and the link between
366 NTA^{W458A} redistribution and pollen tube reception (Fig 5) suggests that NTA
367 accumulation at the pollen tube/synergid interface is important for the intercellular
368 communication process that occurs between the pollen tube and synergids. In *nta-1*
369 mutants, around 30% of ovules display pollen tube overgrowth and fail to complete
370 double fertilization, but the other 70% are fertilized normally (Kessler et al., 2010). This
371 indicates that NTA is not absolutely required for pollen tube reception, but may function
372 as a modifier of the FER signaling pathway. Since FER signaling in the synergids leads
373 to cell death as pollen tube reception is completed (Huck et al., 2003; Rotman et al.,
374 2003; Escobar-Restrepo et al., 2007), NTA trafficking to the filiform apparatus from
375 could be a mechanism to regulate this death and would thus require sequestration of
376 "toxic" NTA in the Golgi before pollen tube arrival. In order to test this hypothesis, we
377 took advantage of sequence variation leading to differential subcellular localization of
378 MLO proteins to manipulate the subcellular localization of NTA. When expressed in
379 synergids, other proteins from the Arabidopsis MLO family have different subcellular
380 localization patterns, indicating that specific sequences within the MLOs direct them to
381 different parts of the secretory system (Jones and Kessler, 2017). MLO1-GFP localizes
382 in the filiform apparatus region of the synergids when it is ectopically expressed under
383 control of the synergid-specific MYB98 promoter and cannot complement the *nta-1*
384 pollen tube reception phenotype (Jones et al., 2017), also see Fig 6C). Domain swaps

385 between different regions of NTA and MLO1 revealed that the C-terminal cytoplasmic
386 tail including the CaMBD of MLO1 (NTA-MLO1^{CTerm}, see diagram in Fig 6B) was
387 sufficient to direct the fusion protein to the filiform apparatus region of the synergids, in
388 a pattern very similar to MLO1-GFP (Fig 6A-C). Quantification of the GFP signal along
389 the length of the synergids from the chalazal end to the filiform apparatus in the NTA-
390 GFP, NTA-MLO1^{Cterm}-GFP, and MLO1-GFP confirmed that the MLO1 tail was sufficient
391 to move the NTA protein to the filiform apparatus end of the cell (Fig 6D). In all MLO1-
392 GFP and NTA-MLO1^{Cterm}-GFP ovules, the majority of GFP signal was detected in the
393 lower 20-40% of the synergids and most of the signal overlapped with the diffuse FM4-
394 64 staining in the filiform apparatus (Fig 6E). In contrast, NTA-GFP is excluded from the
395 filiform apparatus (Fig 6A and (Jones et al., 2017).
396
397 The successful manipulation of NTA subcellular localization provided a tool for
398 determining the functional relevance of NTA redistribution. We transformed the NTA-
399 MLO1^{CTerm}-GFP construct into *nta-1* plants and used the percentage of unfertilized
400 ovules as a measurement for the ability of the fusion construct to complement the *nta-1*
401 phenotype of unfertilized ovules caused by pollen tube overgrowth (Kessler et al.,
402 2010).Two independent NTA-MLO1^{CTerm}-GFP insertions were able to rescue the *nta-1*
403 phenotype when expressed in synergids (Fig 6F). These data indicate that premature
404 targeting of NTA to the filiform apparatus is not toxic to synergid cells.
405
406
407

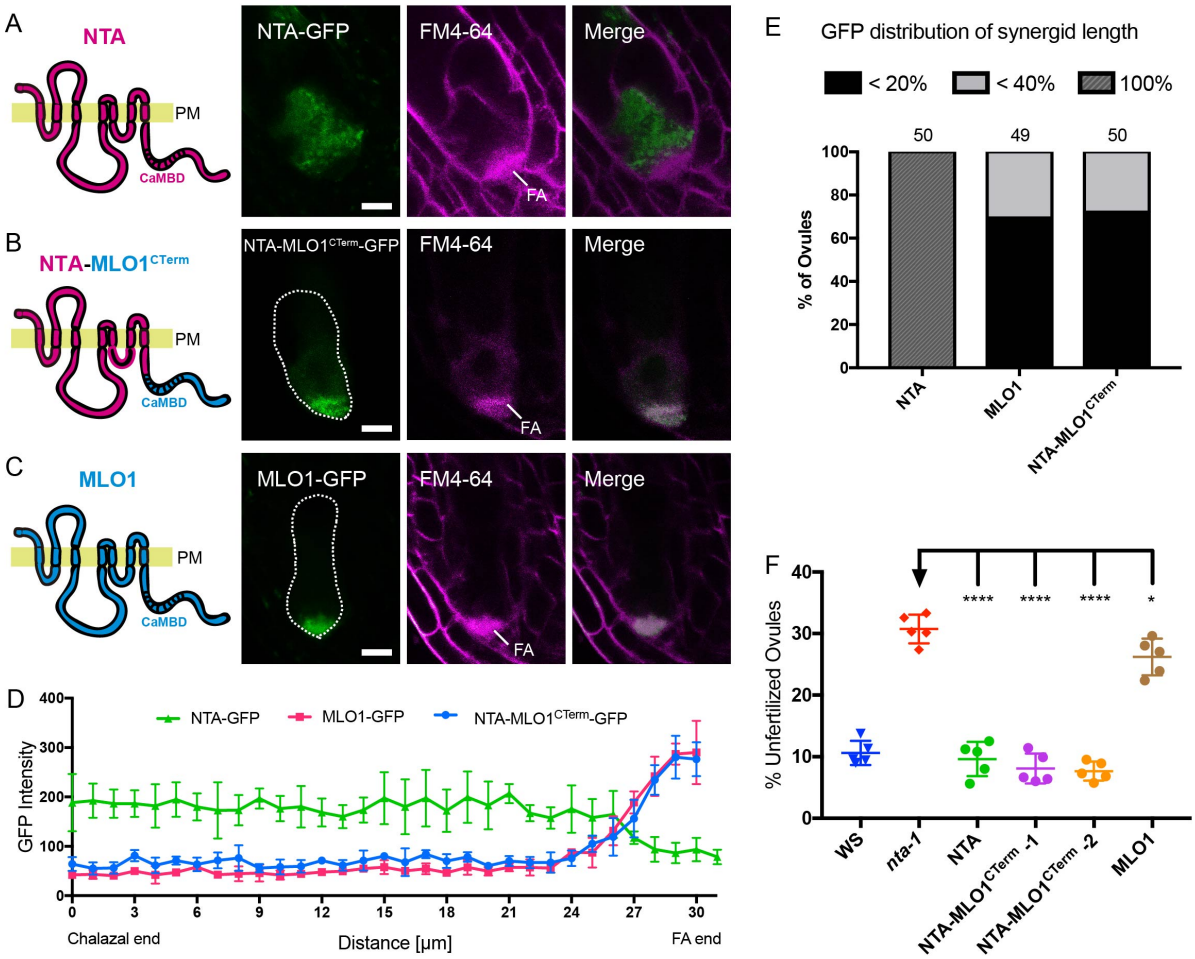

Figure 6. Targeting of NTA to the filiform apparatus region before pollen tube arrival is not toxic to synergid cells. (A-C) Localization patterns of MYB98 promoter-driven MLO-GFP variants (green signal) in synergids of mature virgin ovules stained with FM4-64 (magenta signal) to reveal the outline of the synergid and the filiform apparatus (FA, diffuse magenta signal). (D) Quantification of the GFP intensity of the MLO variants in A-C along the length of the synergids. (E) Percentage of ovules showing MLO-GFP signal throughout the synergids (100% of length), in the micropylar 20% of synergid length that includes the filiform apparatus, and in the region surrounding and including the filiform apparatus (40% of length). (F) Scatter plot of unfertilized ovule percentages in homozygous plants of pMYB98::MLO-GFP in *nta-1* mutants to assess the ability of the MLO-GFP constructs to complement *nta-1*. WS, Wassilewskija. Significance was determined by a Student's *t*-test (****, $P < 0.0001$; *, $P = 0.0281$). Bars = 10 µm.

418 **Discussion**

419 **Synergids respond to a signal from the approaching pollen tube**

420 Successful pollination and production of seeds requires a series of signaling events
421 between the male gametophyte (pollen tube) and both sporophytic and gametophytic
422 cells of the female. In this study, we used live imaging to characterize dynamic
423 subcellular changes that occur in the synergid cells of the female gametophyte in
424 response to the arrival of the pollen tube. We showed that both the NTA protein and
425 endosomes are actively mobilized to the filiform apparatus region where male-female
426 communication occurs during pollen tube reception (Fig 7). Disruption of NTA's CaMBD
427 partially compromised NTA redistribution and function in pollen tube reception, revealing
428 that Ca^{2+} may play a role the synergid response to the signal from the pollen tube.

429

430 The polar accumulation of the RabA1g endosome marker near the filiform apparatus
431 during pollen tube reception suggests a change in synergid secretory system behavior
432 that is triggered by the approaching pollen tube. Our results with the ER, Golgi, TGN,
433 and peroxisome markers indicate that the mobilization of the RabA1g endosomes
434 toward the approaching pollen tube is not just a symptom of FER signaling triggering
435 synergid cell death that leads to mass disruption of subcellular compartments. Trans-
436 Golgi Network/Early endosomes (TGN/EEs) have been shown to be involved in the
437 trafficking of both secretory and endocytic cargo (Viotti et al., 2010). RabA1g is present
438 in endosomes that are highly sensitive to Brefeldin A in roots, suggesting that they could
439 function as recycling endosomes (Geldner et al., 2009). While the resolution of our live
440 imaging system did not allow us to determine whether NTA completely co-localizes with

441 this compartment, it is tempting to speculate that the RabA1g endosomes are mediating
442 the polar movement of NTA to the filiform apparatus region. Alternatively, these
443 endosomes could be transporting other signaling molecules either to or from the filiform
444 apparatus.

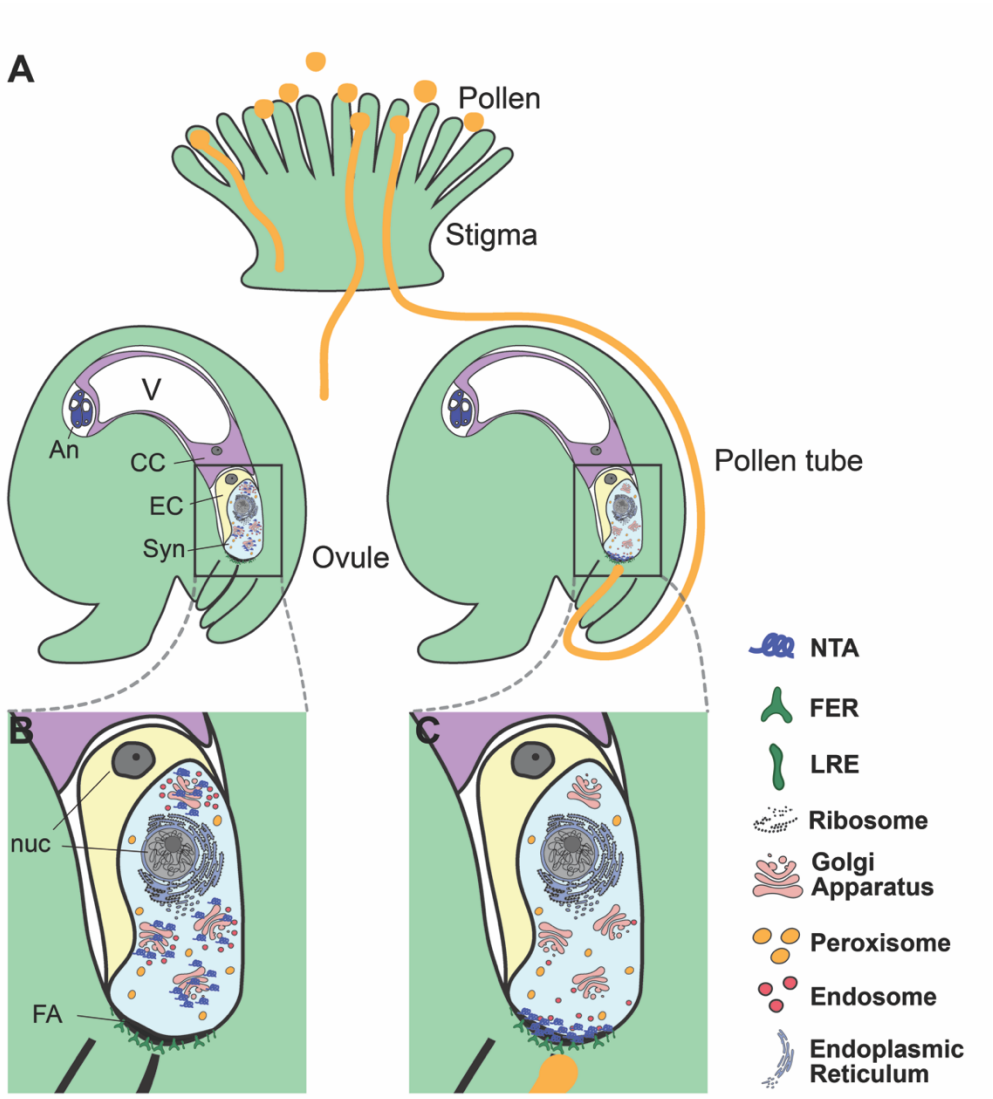

445

446 **Figure 7. Subcellular dynamics in synergids during pollen tube reception.** (A) Pollination
447 using a semi-*in vivo* pollen tube guidance assay. (B) Before pollen tube arrival, NTA is in a
Golgi-associated compartment and endosomes are distributed throughout the synergids. (C)
448 As a pollen tube arrives, NTA and endosomes move toward the filiform apparatus (FA). NTA
redistribution is dependent on signaling from the FER receptor like kinase, which acts in a
complex with LRE. Abbreviations: CC, Central Cell; Syn, Synergid cells; EC, Egg Cell; An,
449 Antipodal cells; nuc, Nucleus; FA, Filiform Apparatus; V, Vacuole.

450 **Signal-mediated protein trafficking**

451 Signal-mediated regulation of protein trafficking is an elegant mechanism to control the
452 delivery of molecules to the precise location where they are needed for critical signaling
453 events that occur over relatively short time frames. Selective protein targeting similar to
454 NTA movement in response to pollen tube arrival has also been observed during cell-to-
455 cell communication between the egg and sperm cells in Arabidopsis. After pollen tube
456 reception and release of the sperm cells, a signal from the sperm and/or the
457 degenerated synergid cell causes the egg cell to secrete EGG CELL 1 (EC1) peptides
458 that have been stored in punctate compartments in the egg cytoplasm toward the sperm
459 cells. The sperm cells perceive the EC1 signal and, in turn, mobilize the gamete
460 fusogen HAPLESS2/GENERATIVE CELL SPECIFIC1 (HAP2/GCS1) from a
461 cytoplasmic compartment to the cell surface (Sprunck et al., 2012). This controlled
462 movement of proteins that have already been translated and stored allows for a quick
463 response that allows the egg and sperm to become activated for fertilization. Likewise,
464 NTA mobilization to the filiform apparatus region of the synergids as the pollen tube
465 arrives could play a role in sending a signal to the pollen tube that leads to the
466 mobilization of pollen tube proteins that allow the pollen tube to rupture and release the
467 sperm cells. For example, proteins that regulate the integrity of the tip of the pollen tube
468 could be quickly delivered after the “arrival” signal from the synergid is perceived.
469 Recent work on the role of the pollen-expressed ANXUR1 and 2 and BUDDHA PAPER
470 SEAL1 and 2 receptor-like kinases in pollen tube tip integrity support this hypothesis.
471 During pollen tube growth through the female tissues, RALF4 and RALF19 peptides that
472 are secreted from pollen tubes act as ligands for ANX1/2 and BPS1/2 to promote tip

473 growth, while RALF34 secreted from the synergids displaces RALF4 and 19 from the
474 receptors leading to subcellular changes that result in pollen tube rupture (Ge et al.,
475 2017).
476
477 **Calcium and NTA movement**
478 Our study revealed that an intact CaMBD facilitates the movement of NTA from the
479 Golgi to the filiform apparatus in response to the stimulus from the approaching pollen
480 tube. This result provides an intriguing link to Ca^{2+} since the polar movement of NTA-
481 GFP to the filiform apparatus region occurs in a similar time frame to $[Ca^{2+}]_{cyto}$ spiking in
482 the synergids during pollen tube reception (Denninger et al., 2014; Ngo et al., 2014).
483 Subcellular Ca^{2+} spiking occurs in plant responses to both biotic and abiotic external
484 stimuli. Notably, Ca^{2+} oscillations occur during pollen tube-synergid interactions, egg-
485 sperm interactions, and in biotrophic interactions between plant cells and both beneficial
486 and harmful microbes (reviewed in (Chen et al., 2015). In most cases, the mechanism
487 for decoding Ca^{2+} spikes into a cellular response is not known, but Ca^{2+}-binding proteins
488 such as calmodulin (CaM) and calmodulin-like proteins could play a role in relaying Ca^{2+}
489 signals (Chin and Means, 2000). In *nta-1* mutants, the $[Ca^{2+}]_{cyto}$ oscillations still occur,
490 but at a lower magnitude than in wild-type synergids, suggesting that NTA could be
491 involved in modulating Ca^{2+} flux (Ngo et al., 2014). The source of Ca^{2+} during these
492 oscillations is not known, but it is possible that NTA regulates Ca^{2+} channels to regulate
493 the flow of Ca^{2+}ions into or out of the apoplast near the filiform apparatus.
494

495 Ca^{2+} has also been linked to regulation of endomembrane trafficking (reviewed in
496 (Himschoot et al., 2017). In animals, calmodulin plays a role in regulating vesicle
497 tethering and fusion (Burgoyne and Clague, 2003), and in plants calmodulin-like
498 proteins are associated with endosomal populations (Ruge et al., 2016). Thus, it is
499 possible that the CaMBD in NTA is critical for the precise targeting of NTA in response
500 to pollen tube arrival. Another mechanism that has been proposed for Ca^{2+}regulation of
501 protein targeting is that electrostatic interactions between Ca^{2+} and anionic
502 phospholipids in specific domains of the plasma membrane regulate vesicle fusion and
503 differential recruitment of proteins to these domains (Simon et al., 2016; Platre et al.,
504 2018). The filiform apparatus of the synergids is distinctive from the plasma membrane
505 in other parts of the synergid and likely has a unique phospholipid composition that
506 could play a role in recruiting NTA to this domain. Whether NTA movement is a cause
507 or consequence of $[Ca^{2+}]_{cyto}$ spiking requires more live imaging experiments at a higher
508 time resolution to determine if NTA redistribution happens before or after the initiation of
509 $[Ca^{2+}]_{cyto}$ spiking.
510

511 **Cell death and pollen tube reception**

512 MLOs were first discovered in barley as powdery mildew resistance genes (Buschges et
513 al., 1997). *mlo* mutants in both monocots and dicots are resistant to powdery mildew
514 infection, indicating that the MLO proteins are required for infection. These mutants also
515 have ectopic cell death, indicating that one function of MLO proteins is to negatively
516 regulate cell death (Panstruga, 2005). Pollen tube reception is catastrophic for both the
517 pollen tube and the receptive synergid cell: both cells die as a result of successful male-

518 female signaling and delivery of the male gametes. The timing of synergid degeneration
519 remains under debate, with some studies suggesting that it occurs upon pollen tube
520 arrival at the synergid and others concluding that it occurs concurrently with pollen tube
521 rupture (Sandaklie-Nikolova et al., 2007; Hamamura et al., 2011; Leydon et al., 2015).
522 Our live imaging experiments with both NTA-GFP and the subcellular compartment
523 reporters suggest that the synergid cells are still alive and regulating their secretory
524 systems up to the point of pollen tube rupture. Given the function of the "powdery
525 mildew" members of the MLO gene family in preventing cell death, it is possible that one
526 role of NTA is to prevent early degeneration of the synergids. An interesting parallel
527 between powdery mildew infection and pollen tube reception is that, in both cases, an
528 MLO protein gets redistributed to the site of interaction with a tip-growing cell. In the
529 powdery mildew system, active transport of proteins and lipids to penetration site leads
530 to membrane remodeling and establishment of the extrahaustorial membrane which
531 separates the plant cytoplasm from the invading fungal hyphae (Huckelhoven and
532 Panstruga, 2011). Although the relationship between the arriving pollen tube and the
533 filiform apparatus has not been established, it is possible that similar reorganization
534 occurs in the filiform apparatus during signaling with the pollen tube. In both cases,
535 perhaps an MLO protein is needed in these special membrane regions to stabilize the
536 cell and prevent precocious cell death. Our result that premature delivery of NTA (in the
537 NTA-MLO1^{CTerm} domain swap construct) to the filiform apparatus region of the cell does
538 not disrupt pollen tube reception is consistent with this hypothesis, since other signaling
539 processes occurring in the synergids during communication with the arriving pollen tube

540 would likely not be triggered by simply moving NTA to the filiform apparatus in the
541 absence of a pollen tube.
542
543 In this study, we showed that signals from an approaching pollen tube trigger the
544 movement of NTA out of the Golgi and to the region of the filiform apparatus and that
545 this redistribution is correlated with pollen tube reception. However, localization of the
546 NTA-MLO1^{CTerm} fusion protein was able to complement the *nta-1* mutant phenotype,
547 indicating that the final localization of the NTA protein may be more important than the
548 active trafficking from the Golgi compartment. Future work will focus on determining the
549 mechanism through which NTA becomes polarly redistributed and on identifying the
550 signals from the pollen tube that lead to important subcellular changes in the synergids
551 during pollen tube reception.
552
553 **Materials and methods**
554 **Plant materials and growth conditions**
555 *Arabidopsis thaliana* lines expressing NTA$_{pro}$::NTA-GFP, MYB98$_{pro}$::NTA-GFP,
556 MYB98$_{pro}$::MLO1-GFP Golgi-associated marker (Man49-mCherry), ER-associated
557 marker (SP-mCherry-HDEL), TGN-associated marker (SYP61-mCherry), peroxisome-
558 associated marker (Peroxisome-mCherry) and recycling endosome-associated marker
559 (mCherry-RabA1g), were generated and described in previous publications (Kessler et
560 al., 2010; Liu et al., 2016; Jones et al., 2017; Jones et al., 2018). Pollen tube marker
561 lines, ACA9::DsRed (Boisson-Dernier et al., 2008) and Lat52::GFP (Palanivelu and
562 Preuss, 2006) were generously provided by Dr. Aurelien Boisson-Dernier and Dr. Ravi

563 Palanivelu. Seeds were sterilized and plated on ½-strength Murashige and Skoog (MS)
564 plates. All plates were sealed and stratified at 4˚C for two days, and then transferred to
565 the growth chamber (long day conditions, 16 h of light and 8 h of dark at 22˚C) for
566 germination and growth. After 5-7 days, seedlings were transplanted to soil. Seeds from
567 transformed lines were sterilized and plated on ½ MS plate with 20 mg/L hygromycin for
568 selection of transgenic seedlings, which were then transplanted to soil and grown in
569 long days.
570
571 **Live Imaging of Pollination Using a Semi-*in vivo* Pollen Tube Guidance Assay**
572 The semi-*in vivo* system of pollen tube reception was modified from (Palanivelu and
573 Preuss, 2006). Approximately 150 µL of pollen germination media (5 mM KCl, 1 mM
574 $MgSO_4$, 0.01% (w/v) H_3BO_3, 5 mM $CaCl_2$, 20% sucrose, 1.5% agarose, and adjusted
575 pH to 7.5 with KOH) was poured into a Glass Bottom Culture Petri Dish (MatTek
576 Corporation, P35G-1.0-20-C) and spread out using a pipette. Pistils were emasculated
577 and 2 d later were hand pollinated with ACA9::DsRed or Lat52::GFP pollen and
578 returned to the growth chamber. Approximately 1 h after pollination, pistils were
579 removed from plants and placed on double sided tape on a glass slide. Stigmas were
580 cut using single-sided razor blade and placed on pollen germination media using
581 forceps. 8-10 ovules were arranged around the cut style and the petri dish was returned
582 to the growth chamber. After 4-6 h, pollen tubes grew through the stigma and style and
583 emerged near the ovules. Imaging commenced when the pollen tubes approached
584 ovules. Time-lapse images were acquired at 5 min intervals by spinning disk confocal
585 microscopy using an Andor Revolution XD platform with a Yokogawa CSU-X1-A1

586 scanner unit mounted on an Olympus IX-83 microscope and a 20X/0.5 NA objective
587 (Olympus). An Andor iXon Ultra 897BV EMCCD camera was used to capture GFP
588 fluorescence (488-nm excitation) and red fluorescent protein (dsRed or mCherry)
589 fluorescence (561-nm excitation).
590
591 For each experimental condition, at least 60 ovules were imaged over the time course
592 from pollen tube approaching the ovule to completion of pollen tube reception (pollen
593 tube rupture to release the sperm cells). Neighboring ovules that did not attract pollen
594 tubes were imaged at the same time and served as controls for photoxicity.
595
596 **Confocal laser scanning microscopy (CLSM)**
597 CLSM to examine MLO variant subcellular localization was performed on ovules
598 dissected 2 d after emasculation. FM4-64 staining was performed according to the
599 protocol described in (Jones et al., 2017). CLSM was done using either a Nikon A1Rsi
600 inverted confocal microscope according to (Yuan and Kessler, 2019) or a Leica SP8
601 upright confocal microscope according to (Jones et al., 2017).
602
603 **Quantification of fluorescence signal intensity**
604 Two-channel images were adjusted for brightness and contrast using Fiji (Schindelin et
605 al., 2012). Then, they were input to NIS-Elements software (Ver. 5.02) to measure the
606 fluorescence signal intensity. A line that spanned from the chalazal end to the filiform
607 apparatus end of the synergid was used for the signal intensity measurements. For a
608 more accurate representation of the total area of the synergid, signal intensities were

609 recorded along the same length line at five parallel position within the synergid cell.
610 Finally, all the measurement data were output as Excel files. Graphs and statistical
611 analysis were performed with Prism software (www.graphpad.com).
612
613 **Video processing**
614 Images were filtered to remove the noise and cropped using Fiji (Version 2.0.0).
615 QuickTime Player (Version 10.5) was used for movie editing and time-lapse analyses.
616
617 **Cloning and Generation of Transgenic Lines**
618 PCR amplification with PHUSION High-Fidelity Polymerase (NEB, M0535S) or Q5 High-
619 Fidelity DNA Polymerase (NEB, M0419S) were used to generate the following
620 constructs in this study. Genes were amplified with primers that had attB1 and attB2
621 sites for recombination via BP reaction into the Gateway-compatible entry vector
622 pDONR207. Full-length NTA entry vectors used in this study was generated as
623 described previously (Jones et al., 2017) . NTA truncations were amplified using NTA
624 full-length entry vector as a template with forward primer NTA-FattB1 and the following
625 reverse primers: NTA450-RattB2 and NTA481-RattB2 (See all primer sequences in
626 Table S1). The NTA^{W458A} point mutation was generated using the same *NTA* template
627 and amplifying two fragments of *NTA* with desired point mutations introduced into the
628 primers: NTA-FattB1 + NTAW458A-R and NTAW458A-F + NTA-RattB2. The two
629 fragments were purified and pasted together with overlaps using a PCR-pasting
630 protocol. The NTA-$MLO1^{CTerm}$ construct was generated using the full-length entry
631 vectors of NTA and MLO1 used in previous study (Jones et al., 2017) as templates and

632 amplifying two fragments of *NTA* and *MLO1* using the two pairs of primers: NTA-FattB1
633 +NTA-R19 and MLO1-F + MLO1-RattB2. The two fragments were purified and pasted
634 together with overlaps using a PCR-pasting protocol. The coding sequence from both
635 truncations and the point mutation and the fusion sequence were fully sequenced in
636 entry vectors. All entries were then recombined via LR reactions into the pMDC83
637 backbone with the $MYB98_{pro}$ (Muller et al., 2016) to drive expression of each NTA
638 variant in synergid cells with a C-terminal GFP fusion.
639
640 For *nta-1* complementation assay and co-localization analyses, expression vectors were
641 transformed into the *Agrobacterium tumefaciens* strain GV3101 and transformed into
642 the *nta-1* mutant background or the Col-0 background (co-localization – Col-0 was
643 stably expressing the Golgi or TGN synergid secretory markers) via the floral-dip
644 method (Bent, 2006). Stable transgenic lines were selected using their respective
645 selections described above. Homozygous T2 lines were used in *nta-1* complementation
646 assay and co-localization imaging in the synergid was done in a T1 analysis.
647
648 ***nta-1* Complementation Assays**
649 3-4 independent insertion lines for each construct were taken to the T2 generation and
650 screened for homozygosity using fluorescence microscopy to ensure transgene
651 expression in synergids of every ovule. Unfertilized vs. fertilized ovule counts from self-
652 pollinated flowers were assessed in at least three plants of each insertion line and
653 compared to *nta-1*, Wassilewskija (Ws-2; wildtype), and the previously published full-
654 length NTA ($MYB98_{pro}$::NTA-GFP in *nta-1* background, (Jones et al., 2017). Ovule

655 counts were statistically analyzed using Prism (www.graphpad.com) with significance
656 determined using a Student's *t*-test. Comparisons of the NTA variants were made to full-
657 length NTA and the *nta-1* mutant.
658

659 **Acknowledgements**

660 We thank Patrick Day for technical assistance and Rachel Flynn and Thomas Davis for
661 helpful discussions and comments on the manuscript. This work was supported by
662 funds from NSF IOS-1733865 to SAK, Purdue University Start-up funds to SAK, and a
663 grant from the Oklahoma Center for the Advancement of Science and Technology
664 #PS14-008 to SAK. Spinning disk confocal microscopy in the Staiger laboratory was
665 supported, in part, by an award from the Office of Science at the US Department of
666 Energy, Physical Biosciences Program, under contract number DE-FG02-09ER15526
667 to CJS.
668

669 **Author Contributions**

670 JY, YJ, DSJ, and SAK conceived and designed the experiments. JY, YJ, DSJ, NL, and
671 WZ performed the experiments. JY, YJ, DSJ, and SAK analyzed the data. JY, YJ, DSJ,
672 and SAK wrote the manuscript, and all authors revised and approved the final
673 manuscript.
674

675 **Competing Interests**

676 The authors declare no competing interests.
677

678 **Supplemental Materials**

679 **Supplementary figure 1.** NTA consistently redistributes to the filiform apparatus region
680 during pollen tube arrival.

681 **Supplementary figure 2.** Subcellular marker behavior during reception of Lat52::GFP
682 labeled pollen tubes.

683 **Supplementary figure 3**. Additional examples of RabA1g endosome markers during
684 pollen tube reception.

685 **Supplementary figure 4.** NTA^{W458A} co-localizes with a Golgi marker in synergid cells.

686 **Supplementary figure 5**. NTA and NTA^{W458A} distribution in the synergid at pollen tube
687 arrival.

688

689 **Movies**

690 **Supplementary movie 1.** NTA-GFP (green signal) redistributes to filiform apparatus
691 region as ACA9::DsRed labeled pollen tube (magenta signal) approaches.

692 **Supplementary movie 2.** NTA-GFP (green signal) redistributes to filiform apparatus
693 region during pollen tube reception (GFP channel only, same movie as S1).

694 **Supplementary movie 3.** Golgi-mCherry signals (magenta signal) are evenly
695 distributed along the length of the synergid as Lat52::GFP labeled pollen tube (green
696 signal) approaches.

697 **Supplementary movie 4.** Golgi-mCherry signals (magenta signal) are evenly
698 distributed along the length of the synergid during pollen tube reception (mCherry
699 channel only, same movie as S3).

700 **Supplementary movie 5.** The trans-Golgi marker SYP61-mCherry (magenta signal) is
701 localized toward the micropyle region of synergid cells both before and after pollen tube
702 (green signal) arrival.
703 **Supplementary movie 6.** The trans-Golgi marker SYP61-mCherry (magenta signal) is
704 localized toward the micropyle region of synergid cells during pollen tube reception
705 (mCherry channel only, same movie as S5).
706 **Supplementary movie 7.** Before and after pollen tube (green signal) arrival, the ER
707 marker SP-mCherry-HDEL (magenta signal) is distributed throughout synergid cells.
708 **Supplementary movie 8.** The ER marker SP-mCherry-HDEL (magenta signal) is
709 distributed throughout synergid cells (mCherry channel only, same movie as S7).
710 **Supplementary movie 9.** The peroxisome marker mCherry-SLK (magenta signal) does
711 not redistribute to the filiform apparatus region after pollen tube (green signal) arrival.
712 **Supplementary movie 10.** The peroxisome marker mCherry-SLK (magenta signal)
713 does not redistribute to the filiform apparatus region during pollen tube reception
714 (mCherry channel only, same movie as S9).
715 **Supplementary movie 11.** RabA1g-mCherry endosome marker (magenta signal)
716 accumulates at the filiform apparatus region in response to pollen tube (green signal)
717 arrival.
718 **Supplementary movie 12.** RabA1g-mCherry endosome marker (magenta signal)
719 accumulates at the filiform apparatus region during pollen tube reception (mCherry
720 channel only, same movie as S11).
721 **Supplementary table 1. List of primers used for cloning.**
722 **Figure 4 Source Data:** Seed count data from NTA truncation and point mutation
723 complementation experiments.

724 **Figure 6 Source Data:** Seed count data from NTA-MLO1^{CTerm} complementation
725 experiments.
726

727

728 ## References

729 **Arazi, T., Baum, G., Snedden, W.A., Shelp, B.J., and Fromm, H.** (1995). Molecular and
730 Biochemical-Analysis of Calmodulin Interactions with the Calmodulin-Binding Domain of
731 Plant Glutamate-Decarboxylase. Plant Physiology **108,** 551-561.
732 **Bent, A.** (2006). Arabidopsis thaliana Floral Dip Transformation Method. In Methods in
733 Molecular Biology, K. Wang, ed (Totowa, NJ: Humana Press Inc.
734 **Boisson-Dernier, A., Frietsch, S., Kim, T.H., Dizon, M.B., and Schroeder, J.I.** (2008). The peroxin
735 loss-of-function mutation abstinence by mutual consent disrupts male-female
736 gametophyte recognition. Curr Biol **18,** 63-68.
737 **Burgoyne, R.D., and Clague, M.J.** (2003). Calcium and calmodulin in membrane fusion. Biochim
738 Biophys Acta **1641,** 137-143.
739 **Buschges, R., Hollricher, K., Panstruga, R., Simons, G., Wolter, M., Frijters, A., van Daelen, R.,**
740 **van der Lee, T., Diergaarde, P., Groenendijk, J., Topsch, S., Vos, P., Salamini, F., and**
741 **Schulze-Lefert, P.** (1997). The barley Mlo gene: a novel control element of plant
742 pathogen resistance. Cell **88,** 695-705.
743 **Capron, A., Gourgues, M., Neiva, L.S., Faure, J.E., Berger, F., Pagnussat, G., Krishnan, A.,**
744 **Alvarez-Mejia, C., Vielle-Calzada, J.P., Lee, Y.R., Liu, B., and Sundaresan, V.** (2008).
745 Maternal Control of Male-Gamete Delivery in Arabidopsis Involves a Putative GPI-
746 Anchored Protein Encoded by the LORELEI Gene. Plant Cell **20,** 3038-3049.
747 **Chen, J., Gutjahr, C., Bleckmann, A., and Dresselhaus, T.** (2015). Calcium signaling during
748 reproduction and biotrophic fungal interactions in plants. Mol Plant **8,** 595-611.
749 **Chin, D., and Means, A.R.** (2000). Calmodulin: a prototypical calcium sensor. Trends Cell Biol
750 **10,** 322-328.
751 **Consonni, C., Humphry, M.E., Hartmann, H.A., Livaja, M., Durner, J., Westphal, L., Vogel, J.,**
752 **Lipka, V., Kemmerling, B., Schulze-Lefert, P., Somerville, S.C., and Panstruga, R.** (2006).
753 Conserved requirement for a plant host cell protein in powdery mildew pathogenesis.
754 Nat Genet **38,** 716-720.
755 **Denninger, P., Bleckmann, A., Lausser, A., Vogler, F., Ott, T., Ehrhardt, D.W., Frommer, W.B.,**
756 **Sprunck, S., Dresselhaus, T., and Grossmann, G.** (2014). Male-female communication
757 triggers calcium signatures during fertilization in Arabidopsis. Nature communications **5,**
758 4645.
759 **Devoto, A., Piffanelli, P., Nilsson, I., Wallin, E., Panstruga, R., von Heijne, G., and Schulze-**
760 **Lefert, P.** (1999). Topology, subcellular localization, and sequence diversity of the Mlo
761 family in plants. J Biol Chem **274,** 34993-35004.
762 **Devoto, A., Hartmann, H.A., Piffanelli, P., Elliott, C., Simmons, C., Taramino, G., Goh, C.S.,**
763 **Cohen, F.E., Emerson, B.C., Schulze-Lefert, P., and Panstruga, R.** (2003). Molecular

764 phylogeny and evolution of the plant-specific seven-transmembrane MLO family. J Mol
765 Evol **56,** 77-88.
766 **Drews, G.N., and Yadegari, R.** (2002). Development and function of the angiosperm female
767 gametophyte. Annu Rev Genet **36,** 99-124.
768 **Escobar-Restrepo, J.M., Huck, N., Kessler, S., Gagliardini, V., Gheyselinck, J., Yang, W.C., and**
769 **Grossniklaus, U.** (2007). The FERONIA receptor-like kinase mediates male-female
770 interactions during pollen tube reception. Science **317,** 656-660.
771 **Ge, Z., Bergonci, T., Zhao, Y., Zou, Y., Du, S., Liu, M.C., Luo, X., Ruan, H., Garcia-Valencia, L.E.,**
772 **Zhong, S., Hou, S., Huang, Q., Lai, L., Moura, D.S., Gu, H., Dong, J., Wu, H.M.,**
773 **Dresselhaus, T., Xiao, J., Cheung, A.Y., and Qu, L.J.** (2017). Arabidopsis pollen tube
774 integrity and sperm release are regulated by RALF-mediated signaling. Science **358,**
775 1596-1600.
776 **Geldner, N., Denervaud-Tendon, V., Hyman, D.L., Mayer, U., Stierhof, Y.D., and Chory, J.**
777 (2009). Rapid, combinatorial analysis of membrane compartments in intact plants with a
778 multicolor marker set. Plant J **59,** 169-178.
779 **Hamamura, Y., Nagahara, S., and Higashiyama, T.** (2012). Double fertilization on the move.
780 Curr Opin Plant Biol **15,** 70-77.
781 **Hamamura, Y., Nishimaki, M., Takeuchi, H., Geitmann, A., Kurihara, D., and Higashiyama, T.**
782 (2014). Live imaging of calcium spikes during double fertilization in Arabidopsis. Nat
783 Commun **5,** 4722.
784 **Hamamura, Y., Saito, C., Awai, C., Kurihara, D., Miyawaki, A., Nakagawa, T., Kanaoka, M.M.,**
785 **Sasaki, N., Nakano, A., Berger, F., and Higashiyama, T.** (2011). Live-cell imaging reveals
786 the dynamics of two sperm cells during double fertilization in Arabidopsis thaliana. Curr
787 Biol **21,** 497-502.
788 **Himschoot, E., Pleskot, R., Van Damme, D., and Vanneste, S.** (2017). The ins and outs of Ca(2+)
789 in plant endomembrane trafficking. Curr Opin Plant Biol **40,** 131-137.
790 **Huang, B.-Q., and Russell, S.D.** (1992). Female Germ Unit: Organization, Isolation, and Function
791 **140,** 233-293.
792 **Huck, N., Moore, J.M., Federer, M., and Grossniklaus, U.** (2003). The Arabidopsis mutant
793 feronia disrupts the female gametophytic control of pollen tube reception.
794 Development **130,** 2149-2159.
795 **Huckelhoven, R., and Panstruga, R.** (2011). Cell biology of the plant-powdery mildew
796 interaction. Curr Opin Plant Biol **14,** 738-746.
797 **Iwano, M., Ngo, Q.A., Entani, T., Shiba, H., Nagai, T., Miyawaki, A., Isogai, A., Grossniklaus, U.,**
798 **and Takayama, S.** (2012). Cytoplasmic Ca2+ changes dynamically during the interaction
799 of the pollen tube with synergid cells. Development **139,** 4202-4209.
800 **Johnson, M.A., Harper, J.F., and Palanivelu, R.** (2019). A Fruitful Journey: Pollen Tube
801 Navigation from Germination to Fertilization. Annu Rev Plant Biol.
802 **Jones, D.S., and Kessler, S.A.** (2017). Cell type-dependent localization of MLO proteins. Plant
803 Signal Behav **12**.
804 **Jones, D.S., Yuan, J., Smith, B.E., Willoughby, A.C., Kumimoto, E.L., and Kessler, S.A.** (2017).
805 MILDEW RESISTANCE LOCUS O Function in Pollen Tube Reception Is Linked to Its
806 Oligomerization and Subcellular Distribution. Plant Physiol **175,** 172-185.

807 **Jones, D.S., Liu, X., Willoughby, A.C., Smith, B.E., Palanivelu, R., and Kessler, S.A.** (2018).
808 Cellular distribution of secretory pathway markers in the haploid synergid cells of
809 Arabidopsis thaliana. Plant J **94,** 192-202.
810 **Kessler, S.A., and Grossniklaus, U.** (2011). She's the boss: signaling in pollen tube reception.
811 Curr Opin Plant Biol **14,** 622-627.
812 **Kessler, S.A., Shimosato-Asano, H., Keinath, N.F., Wuest, S.E., Ingram, G., Panstruga, R., and**
813 **Grossniklaus, U.** (2010). Conserved molecular components for pollen tube reception
814 and fungal invasion. Science **330,** 968-971.
815 **Kim, M.C., Panstruga, R., Elliott, C., Muller, J., Devoto, A., Yoon, H.W., Park, H.C., Cho, M.J.,**
816 **and Schulze-Lefert, P.** (2002a). Calmodulin interacts with MLO protein to regulate
817 defence against mildew in barley. Nature **416,** 447-451.
818 **Kim, M.C., Lee, S.H., Kim, J.K., Chun, H.J., Choi, M.S., Chung, W.S., Moon, B.C., Kang, C.H.,**
819 **Park, C.Y., Yoo, J.H., Kang, Y.H., Koo, S.C., Koo, Y.D., Jung, J.C., Kim, S.T., Schulze-**
820 **Lefert, P., Lee, S.Y., and Cho, M.J.** (2002b). Mlo, a modulator of plant defense and cell
821 death, is a novel calmodulin-binding protein. Isolation and characterization of a rice Mlo
822 homologue. J Biol Chem **277,** 19304-19314.
823 **Kusch, S., Pesch, L., and Panstruga, R.** (2016). Comprehensive Phylogenetic Analysis Sheds Light
824 on the Diversity and Origin of the MLO Family of Integral Membrane Proteins. Genome
825 Biol Evol **8,** 878-895.
826 **Leshem, Y., Johnson, C., and Sundaresan, V.** (2013). Pollen tube entry into the synergid cell of
827 Arabidopsis is observed at a site distinct from the filiform apparatus. Plant reproduction
828 **26,** 93-99.
829 **Leydon, A.R., Tsukamoto, T., Dunatunga, D., Qin, Y., Johnson, M.A., and Palanivelu, R.** (2015).
830 Pollen Tube Discharge Completes the Process of Synergid Degeneration That Is Initiated
831 by Pollen Tube-Synergid Interaction in Arabidopsis. Plant Physiol **169,** 485-496.
832 **Li, C., Yeh, F.L., Cheung, A.Y., Duan, Q., Kita, D., Liu, M.C., Maman, J., Luu, E.J., Wu, B.W.,**
833 **Gates, L., Jalal, M., Kwong, A., Carpenter, H., and Wu, H.M.** (2015).
834 Glycosylphosphatidylinositol-anchored proteins as chaperones and co-receptors for
835 FERONIA receptor kinase signaling in Arabidopsis. Elife **4**.
836 **Lindner, H., Kessler, S.A., Müller, L.M., Shimosato-Asano, H., Boisson-Dernier, A., and**
837 **Grossniklaus, U.** (2015). TURAN and EVAN mediate pollen tube reception in Arabidopsis
838 synergids through protein glycosylation. PLoS Biol **13,** e1002139.
839 **Liu, X., Castro, C., Wang, Y., Noble, J., Ponvert, N., Bundy, M., Hoel, C., Shpak, E., and**
840 **Palanivelu, R.** (2016). The Role of LORELEI in Pollen Tube Reception at the Interface of
841 the Synergid Cell and Pollen Tube Requires the Modified Eight-Cysteine Motif and the
842 Receptor-Like Kinase FERONIA. Plant Cell **28,** 1035-1052.
843 **Mansfield, S.G., Briarty, L.G., and Erni, S.** (1991). Early embryogenesis in Arabidopsis thaliana. I.
844 The mature embryo sac. Canadian Journal of Botany **69,** 447-460.
845 **Muller, L.M., Lindner, H., Pires, N.D., Gagliardini, V., and Grossniklaus, U.** (2016). A subunit of
846 the oligosaccharyltransferase complex is required for interspecific gametophyte
847 recognition in Arabidopsis. Nat Commun **7,** 10826.
848 **Naramoto, S.** (2017). Polar transport in plants mediated by membrane transporters: focus on
849 mechanisms of polar auxin transport. Curr Opin Plant Biol **40,** 8-14.

850 **Ngo, Q.A., Vogler, H., Lituiev, D.S., Nestorova, A., and Grossniklaus, U.** (2014). A Calcium
851 Dialog Mediated by the FERONIA Signal Transduction Pathway Controls Plant Sperm
852 Delivery. Dev Cell **29,** 491-500.
853 **Okuda, S., Tsutsui, H., Shiina, K., Sprunck, S., Takeuchi, H., Yui, R., Kasahara, R.D., Hamamura,**
854 **Y., Mizukami, A., Susaki, D., Kawano, N., Sakakibara, T., Namiki, S., Itoh, K., Otsuka, K.,**
855 **Matsuzaki, M., Nozaki, H., Kuroiwa, T., Nakano, A., Kanaoka, M.M., Dresselhaus, T.,**
856 **Sasaki, N., and Higashiyama, T.** (2009). Defensin-like polypeptide LUREs are pollen tube
857 attractants secreted from synergid cells. Nature **458,** 357-361.
858 **Palanivelu, R., and Preuss, D.** (2006). Distinct short-range ovule signals attract or repel
859 Arabidopsis thaliana pollen tubes in vitro. BMC Plant Biol **6,** 7.
860 **Panstruga, R.** (2005). Serpentine plant MLO proteins as entry portals for powdery mildew fungi.
861 Biochem Soc Trans **33,** 389-392.
862 **Petrasek, J., Mravec, J., Bouchard, R., Blakeslee, J.J., Abas, M., Seifertova, D., Wisniewska, J.,**
863 **Tadele, Z., Kubes, M., Covanova, M., Dhonukshe, P., Skupa, P., Benkova, E., Perry, L.,**
864 **Krecek, P., Lee, O.R., Fink, G.R., Geisler, M., Murphy, A.S., Luschnig, C., Zazimalova, E.,**
865 **and Friml, J.** (2006). PIN proteins perform a rate-limiting function in cellular auxin efflux.
866 Science **312,** 914-918.
867 **Platre, M.P., Noack, L.C., Doumane, M., Bayle, V., Simon, M.L.A., Maneta-Peyret, L., Fouillen,**
868 **L., Stanislas, T., Armengot, L., Pejchar, P., Caillaud, M.C., Potocky, M., Copic, A.,**
869 **Moreau, P., and Jaillais, Y.** (2018). A Combinatorial Lipid Code Shapes the Electrostatic
870 Landscape of Plant Endomembranes. Dev Cell **45,** 465-480 e411.
871 **Rotman, N., Rozier, F., Boavida, L., Dumas, C., Berger, F., and Faure, J.E.** (2003). Female control
872 of male gamete delivery during fertilization in Arabidopsis thaliana. Curr Biol **13,** 432-
873 436.
874 **Ruge, H., Flosdorff, S., Ebersberger, I., Chigri, F., and Vothknecht, U.C.** (2016). The calmodulin-
875 like proteins AtCML4 and AtCML5 are single-pass membrane proteins targeted to the
876 endomembrane system by an N-terminal signal anchor sequence. J Exp Bot **67,** 3985-
877 3996.
878 **Salanenka, Y., Verstraeten, I., Lofke, C., Tabata, K., Naramoto, S., Glanc, M., and Friml, J.**
879 (2018). Gibberellin DELLA signaling targets the retromer complex to redirect protein
880 trafficking to the plasma membrane. Proc Natl Acad Sci U S A **115,** 3716-3721.
881 **Sandaklie-Nikolova, L., Palanivelu, R., King, E.J., Copenhaver, G.P., and Drews, G.N.** (2007).
882 Synergid cell death in Arabidopsis is triggered following direct interaction with the
883 pollen tube. Plant Physiol **144,** 1753-1762.
884 **Schindelin, J., Arganda-Carreras, I., Frise, E., Kaynig, V., Longair, M., Pietzsch, T., Preibisch, S.,**
885 **Rueden, C., Saalfeld, S., Schmid, B., Tinevez, J.Y., White, D.J., Hartenstein, V., Eliceiri,**
886 **K., Tomancak, P., and Cardona, A.** (2012). Fiji: an open-source platform for biological-
887 image analysis. Nat Methods **9,** 676-682.
888 **Simon, M.L., Platre, M.P., Marques-Bueno, M.M., Armengot, L., Stanislas, T., Bayle, V.,**
889 **Caillaud, M.C., and Jaillais, Y.** (2016). A PtdIns(4)P-driven electrostatic field controls cell
890 membrane identity and signalling in plants. Nat Plants **2,** 16089.
891 **Sprunck, S., Rademacher, S., Vogler, F., Gheyselinck, J., Grossniklaus, U., and Dresselhaus, T.**
892 (2012). Egg cell-secreted EC1 triggers sperm cell activation during double fertilization.
893 Science **338,** 1093-1097.

894 **Stoorvogel, W., Strous, G.J., Geuze, H.J., Oorschot, V., and Schwartz, A.L.** (1991). Late
895 endosomes derive from early endosomes by maturation. Cell **65,** 417-427.
896 **Takeuchi, H., and Higashiyama, T.** (2016). Tip-localized receptors control pollen tube growth
897 and LURE sensing in Arabidopsis. Nature **531,** 245-248.
898 **Viotti, C., Bubeck, J., Stierhof, Y.D., Krebs, M., Langhans, M., van den Berg, W., van Dongen,**
899 **W., Richter, S., Geldner, N., Takano, J., Jurgens, G., de Vries, S.C., Robinson, D.G., and**
900 **Schumacher, K.** (2010). Endocytic and secretory traffic in Arabidopsis merge in the
901 trans-Golgi network/early endosome, an independent and highly dynamic organelle.
902 Plant Cell **22,** 1344-1357.
903 **Wang, T., Liang, L., Xue, Y., Jia, P.F., Chen, W., Zhang, M.X., Wang, Y.C., Li, H.J., and Yang, W.C.**
904 (2016). A receptor heteromer mediates the male perception of female attractants in
905 plants. Nature **531,** 241-244.
906 **Yamada, M., Miyawaki, A., Saito, K., Nakajima, T., Yamamoto-Hino, M., Ryo, Y., Furuichi, T.,**
907 **and Mikoshiba, K.** (1995). The calmodulin-binding domain in the mouse type 1 inositol
908 1,4,5-trisphosphate receptor. Biochem J **308 (Pt 1),** 83-88.
909 **Yang, T., and Poovaiah, B.** (2003). Calcium/calmodulin-mediated signal network in plants.
910 Trends in plant science **8,** 505-512.
911 **Yuan, J., and Kessler, S.A.** (2019). A genome-wide association study reveals a novel regulator of
912 ovule number and fertility in Arabidopsis thaliana. PLoS Genet **15,** e1007934.
913

914
915
916 **Figure Legends**

917 **Figure 1. NTA redistributes to the filiform apparatus region as the pollen tube**
918 **approaches.** (A) Diagram of a mature *Arabidopsis thaliana* ovule and embryo sac,
919 modified from Jones et al, 2018. (B, C) Live imaging of pollen tube (PT) reception using
920 NTA-GFP labeled synergids (green signal) and ACA9::DsRed pollen tubes (magenta
921 signal). (B) NTA-GFP redistribution occurred in ovules that attracted a pollen tube
922 (ovules with white stars), while NTA-GFP redistribution did not occur in ovules without
923 pollen tube attraction (ovules with green stars). (C) Time-lapse imaging of NTA-GFP
924 movement during pollen tube reception. NTA-GFP before (ovules with yellow stars) and
925 after (ovules with blue stars) the PT resumes growth after initial arrival at the filiform
926 apparatus. (D) Quantification of NTA-GFP signal before (yellow starred ovule) and after

927 (blue starred ovule) pollen tube arrival. Synergid cell from chalazal end to filiform
928 apparatus (FA) end was defined from 0 to 33 μm in length. (E) Quantification of the
929 percentage of ovules with NTA redistribution under different experimental conditions.
930 Bars=50μm (A, C). CC, Central Cell; Syn, Synergid Cells; EC, Egg Cell; An, Antipodal
931 cells; FA, Filiform Apparatus; PT, Pollen Tube.
932
933 **Figure 2. The Golgi marker is randomly distributed throughout synergids during**
934 **pollen tube reception.** (A) NTA-GFP (green signal) and Golgi-mCherry signals
935 (magenta signal) are evenly distributed along the length of the synergid and co-localized
936 within synergid cells before pollen tube arrival. (B) After pollen tube arrival, NTA-GFP
937 redistributed to FA region, but Golgi-mCherry did not redistribute to FA. (C) Live imaging
938 of Golgi-mCherry during reception of Lat52::GFP labeled pollen tubes. (D)
939 Quantification of Golgi-mCherry signal along the length of synergids before (ovule with
940 yellow star in C) and after (ovule with blue star in C) pollen tube arrival. Bars=30μm (A-
941 B), 50μm (C). Syn, Synergid cells, FA, Filiform Apparatus.
942
943 **Figure 3. Endosome marker polarly accumulates toward filiform apparatus during**
944 **pollen tube reception.** (A) Rab-mCherry endosome marker (magenta signal)
945 accumulates at the FA region in response to pollen tube arrival (ovule with white star).
946 (B) Higher magnification of the micropylar region of starred ovule in (red box in panel A).
947 (C) Timing of Rab-mCherry polar accumulation during pollen tube arrival (ovules with
948 stars). (D) Quantification of Rab-mCherry signal along the length of synergids during
949 pollen tube reception. Bars=50μm. (E) Quantification of ovule percentage with

950 endosome marker throughout the synergids (gray bars) or with polar accumulation near
951 the filiform apparatus (black bars). CC, Central Cell; EC, Egg Cell; Syn, Synergid Cells;
952 FA, Filiform Apparatus; PT, Pollen Tube.
953
954 **Figure 4. Analysis of NTA variants expressed in synergids of *nta-1*.** (A) Diagram of
955 the NTA protein with variant positions indicated. The yellow bar represents a lipid
956 bilayer, with the N-terminal extension predicted to be outside the membrane. (B)
957 Complementation analysis of NTA variants in T2 plants homozygous for
958 $MYB98_{pro}$::NTA(variant)-GFP constructs in *nta-1* mutants. (C-F) NTA (variant)-GFP
959 (green) distribution in synergid cells of unfertilized ovules merged with FM4-64
960 (magenta). Bars = 10 µm. Adjusted P values from a Student's *t*-test are as follows: ****
961 indicates $P < 0.0001$; *** indicates $P = 0.001$ to 0.0001($P = 0.0009$ when compare
962 between NTA and $NTA^{\Delta 450}$; $P = 0.0005$ when compare between NTA and NTA^{W458A});
963 and ns indicates $P = 0.0633$. FA, Filiform Apparatus.
964
965 **Figure 5. A point mutation in the CaMBD (NTA^{W458A}) affects redistribution and**
966 **pollen tube reception.** (A) NTA^{W458A} has 3 different localization patterns in response to
967 PT arrival under semi *in-vivo* conditions. (B) Quantification of GFP signal intensity in
968 NTA^{W458A} synergids during pollen tube reception. (C) Analysis of NTA^{W458A}-GFP
969 distribution patterns in ovules with successful (PT bursting) and unsuccessful (no PT or
970 PT overgrowth (PT OG)) pollen tube reception. Bar=50 µm (B).
971

972 **Figure 6. Targeting of NTA to the filiform apparatus region before pollen tube arrival**
973 **is not toxic to synergid cells.** (A-C) Localization patterns of MYB98 promoter-driven
974 MLO-GFP variants (green signal) in synergids of mature virgin ovules stained with FM4-
975 64 (magenta signal) to reveal the outline of the synergid and the filiform apparatus (FA,
976 diffuse magenta signal). (D) Quantification of the GFP intensity of the MLO variants in A-
977 C along the length of the synergids. (E) Percentage of ovules showing MLO-GFP signal
978 throughout the synergids (100% of length), in the micropylar 20% of synergid length that
979 includes the filiform apparatus, and in the region surrounding and including the filiform
980 apparatus (40% of length). (F) Scatter plot of unfertilized ovule percentages in
981 homozygous plants of pMYB98::MLO-GFP in *nta-1* mutants to assess the ability of the
982 MLO-GFP constructs to complement *nta-1*. WS, Wassilewskija. Significance was
983 determined by a Student's *t*-test (****, $P < 0.0001$; *, $P = 0.0281$). Bars = 10 µm.
984
985 **Figure 7. Subcellular dynamics in synergids during pollen tube reception.** (A)
986 Pollination using a semi-*in vivo* pollen tube guidance assay. (B) Before pollen tube
987 arrival, NTA is in a Golgi-associated compartment and endosomes are distributed
988 throughout the synergids. (C) As a pollen tube arrives, NTA and endosomes move
989 toward the filiform apparatus (FA). NTA redistribution is dependent on signaling from
990 the FER receptor like kinase, which acts in a complex with LRE. Abbreviations: CC,
991 Central Cell; Syn, Synergid cells; EC, Egg Cell; An, Antipodal cells; nuc, Nucleus; FA,
992 Filiform Apparatus; V, Vacuole.
993
994